Received: 25 October 2021 | Revised: 28 April 2022 | Accepted: 12 May 2022

DOI: 10.1111/mec.16538

ORIGINAL ARTICLE

MOLECULAR ECOLOGY WILEY

The road not taken: Evolution of tetrodotoxin resistance in the Sierra garter snake (*Thamnophis couchii*) by a path less travelled

Jessica S. Reimche[1,2] | Robert E. del Carlo[3,4] | Edmund D. Brodie Jr[5] | Joel W. McGlothlin[6] | Karen Schlauch[7] | Michael E. Pfrender[8] | Edmund D. Brodie III[9] | Normand Leblanc[3,4] | Chris R. Feldman[1,2]

[1]Department of Biology, University of Nevada, Reno, Nevada, USA

[2]Program in Ecology, Evolution, and Conservation Biology, University of Nevada, Reno, Nevada, USA

[3]Department of Pharmacology and Physiology, University of Nevada, Reno, Nevada, USA

[4]Program in Cellular and Molecular Pharmacology and Physiology, University of Nevada, Reno, Nevada, USA

[5]Department of Biology, Utah State University, Logan, Utah, USA

[6]Department of Biological Sciences, Virginia Tech, Blacksburg, Virginia, USA

[7]Desert Research Institute, Reno, Nevada, USA

[8]Department of Biological Sciences, University of Notre Dame, Notre Dame, Indiana, USA

[9]Department of Biology, University of Virginia, Charlottesville, Virginia, USA

Correspondence
Chris R. Feldman, Department of Biology, University of Nevada, Reno, 1664 N. Virginia St. (MS 0314), Reno, NV 89557, USA.
Email: ophis@unr.edu

Funding information
National Institutes of Health, Grant/Award Number: R01-HL146054; National Science Foundation, Grant/Award Number: DEB-0922216, DEB-1034686, DEB-1601296 and IOS-1355221

Handling Editor: SUHUA SHI

Abstract

The repeated evolution of tetrodotoxin (TTX) resistance provides a model for testing hypotheses about the mechanisms of convergent evolution. This poison is broadly employed as a potent antipredator defence, blocking voltage-gated sodium channels (Na_v) in muscles and nerves, paralysing and sometimes killing predators. Resistance in taxa bearing this neurotoxin and a few predators appears to come from convergent replacements in specific Na_v residues that interact with TTX. This stereotyped genetic response suggests molecular and phenotypic evolution may be constrained and predictable. Here, we investigate the extent of mechanistic convergence in garter snakes (*Thamnophis*) that prey on TTX-bearing newts (*Taricha*) by examining the physiological and genetic basis of TTX resistance in the Sierra garter snake (*Th. couchii*). We characterize variation in this predatory adaptation across populations at several biological scales: whole-animal TTX resistance; skeletal muscle resistance; functional genetic variation in three Na_v encoding loci; and levels of gene expression for one of these loci. We found *Th. couchii* possess extensive geographical variation in resistance at the whole-animal and skeletal muscle levels. As in other *Thamnophis*, resistance at both levels is highly correlated, suggesting convergence across the biological levels linking organism to organ. However, *Th. couchii* shows no functional variation in Na_v loci among populations or difference in candidate gene expression. Local variation in TTX resistance in *Th. couchii* cannot be explained by the same relationship between genotype and phenotype seen in other taxa. Thus, historical contingencies may lead different species of *Thamnophis* down alternative routes to local adaptation.

KEYWORDS
adaptation, evolutionary genetics, gene expression, muscle physiology, sodium channels (Na_v), tetrodotoxin (TTX)

1 | INTRODUCTION

Convergent evolution, or the independent origin of similar phenotypes in distinct lineages, is one of the most remarkable features of biodiversity (Agrawal, 2017; Losos, 2011). Striking examples of convergence, from replicated mutations in microbial lines (Cooper et al., 2003; Woods et al., 2006), to the repeated evolution of butterfly wing patterns (Li et al., 2019; Supple et al., 2013), to recurrent evolution of ecomorphologies in lizards (Losos et al., 1998; Mahler et al., 2013), demonstrate the pervasiveness of repeated

evolution across the tree of life (Conway-Morris, 2003; Cowen, 2013; Losos, 2017; McGhee, 2011). What remain less clear, however, are the underlying causes of convergent evolution (Agrawal, 2017; Losos, 2011, 2017; Stayton, 2015; Storz, 2016). Does convergent evolution demonstrate the primacy of natural selection in fitting organisms optimally to their environment, or does convergence reveal that functional and genetic constraints channel phenotypic evolution into a limited number of outcomes? Determining the general principles surrounding convergent evolution remains a central challenge of evolutionary biology (Agrawal, 2017; Conway-Morris, 2003; Losos, 2011, 2017; McGhee, 2011).

Progress understanding the ultimate causes of convergence will come from careful examination of the proximate mechanisms of repeated evolution. To this end, an integrative approach is needed to decompose the levels of organization at which convergence occurs (Agrawal, 2017; Losos, 2017). We tend to look for convergence at the phenotypic surface, but exploring the inner workings of the organismal machine that produced the phenotype may expose convergent evolution at one organizational level but not another. For example, convergence in animal performance might be generated by the same physiological response, but accomplished by different proteins, or by the same protein that is altered in different ways (e.g., Davis et al., 2004; Hindle, 2020). These patterns of multilevel convergence present an opportunity to evaluate how constraint and adaptation shape phenotypes at different levels, and with it the picture of predictability (Agrawal, 2017; Losos, 2017). If evolution is shaped by constraints at the protein level, then we expect convergent adaptation to occur at the molecular level (Feldman et al., 2012; Miller et al., 2006; Stern, 2013; Storz, 2016; Weinreich et al., 2006). On the other hand, selection may simply work with a variety of materials at any given level (Jacob, 1977), so that we see convergence at higher organizational scales, but divergence in the physiological or molecular underpinnings of traits (Christin et al., 2010; Losos, 2011; Maynard Smith et al., 1985; Wake, 1991).

The repeated evolution of toxin resistance in chemically mediated systems may be ideal for studying convergence because chemical weapons (defensive and offensive) are ubiquitous in the natural world and provide well-defined selection pressures (Brodie & Brodie, 2015; Dobler et al., 2019; Feldman et al., 2016; Harris & Arbuckle, 2016). In addition, toxin resistance exemplifies the multilevel, integrated construction of a phenotype that appears to converge. Resistance to a toxin is a readily observable adaptation at an organismal level, but an organism might deal with a toxin in a variety of ways (Arbuckle et al., 2017; Brodie, 2009). Many toxins have known molecular targets, and resistance might evolve through changes to those binding sites, changes in the expression of different protein isoforms, saturation of receptors in target tissues, or simply binding and blocking of a toxin (Dobler et al., 2019; ffrench-Constant, 1994; McCabe & Mackessy, 2017; Tarvin et al., 2016; Ujvari et al., 2015). Here we examine the convergent evolution of tetrodotoxin (TTX) resistance in a predator–prey system. We take a hierarchical approach to studying convergence, examining the degree of similarity in multiple underlying levels that make up the adaptation at the organismal level.

TTX is a neurotoxin used by nearly 150 animal species as a powerful defensive poison (e.g., pufferfishes, newts) or potent predatory venom (e.g., certain flatworms, blue-ringed octopus) (Lorentz et al., 2016). TTX binds to the outer pore of voltage-gated sodium channels (Na_v) in excitable cells, blocking the influx of Na^+ across the cell membrane, thereby halting nerve impulses and muscle contractions (Fozzard & Lipkind, 2010; Hille, 2001). At an organismal level, animals that ingest or are injected with TTX suffer paralysis, respiratory failure and often death (Abal et al., 2017; Brodie, 1968). Despite the fact that TTX is one of the most lethal natural poisons (Lorentz et al., 2016), dozens of species across 13 phyla have independently evolved resistance to this toxin (Lorentz et al., 2016; Bucciarelli et al., 2021).

Resistance to TTX appears to be achieved through molecular changes in Na_v channels (Du et al., 2009; Feldman et al., 2012; Geffeney et al., 2005; Geffeney et al., 2019; Hanifin & Gilly, 2015; Jost et al., 2008; McGlothlin et al., 2014; Vaelli et al., 2020; Venkatesh et al., 2005; Yoshida, 1994). In reptiles, nine functional Na_v channels are encoded by the *SCN* gene family (Widmark et al., 2011; Zakon et al., 2011). Each *SCN* paralogue codes for a unique α-subunit protein ($Na_v1.1$–$Na_v1.9$) with specific expression profiles primarily in one organ or tissue type, such as skeletal muscle, cardiac muscle, and the nerves of the central and peripheral nervous system, and with minor expression in other tissues (Catterall, 2012; Goldin, 2001; Zakon, 2012). These α-subunits consist of four domains (DI–DIV) that fold together to form a membrane-spanning channel with an inner and outer pore that allow selective permeation of Na^+ ions (Goldin, 2001; Hille, 2001). The outer pore is formed by four structures called P-loops that contain a suite of amino acids that selectively filter Na^+ but also serve as the binding site of TTX (Fozzard & Lipkind, 2010; Goldin, 2001; Hille, 2001). TTX occludes the outer pore through steric attraction and several molecular bonds with residues of the P-loop, thereby blocking the passage of Na^+ ions through the channel (Choudhary et al., 2003; Fozzard & Lipkind, 2010; Terlau et al., 1991). Two Na_v channels are known to be natively resistant to TTX, each due to a single (ancestral) replacement at a critical P-loop site in domain I: $Na_v1.5$ in cardiac muscle and $Na_v1.9$ in sensory nerves (Akopian et al., 1996; Backx et al., 1992; Benn et al., 2001). The sensory neuron sodium channel $Na_v1.8$ also gained a modest degree of TTX resistance in amniotes through an ancestral mutation at a different P-loop site in domain 1 (Perry et al., 2018). In mammals, this channel then gained high resistance through a mutation at the same site as in $Na_v1.5$ and $Na_v1.9$ (Perry et al., 2018), while in reptiles, TTX resistance in $Na_v1.8$ may vary considerably, with some lineages possessing just the one ancestral replacement in domain I (e.g., birds and turtles) and others gaining mutations at other key P-loop sites (e.g., some snakes and lizards) (Perry et al., 2018.) In addition, three other Na_v channels are protected by the blood–brain barrier, and thus sheltered from effects of TTX: $Na_v1.1$–$Na_v1.3$ of the central nervous system

(Goldin, 2001, 2002; Zimmer, 2010). Thus, heightened resistance is expected to occur via substitutions in the remaining sensitive paralogues that are exposed to TTX: $Na_v1.4$ in skeletal muscle, and $Na_v1.6$ and 1.7 in peripheral nerves (Brodie& Brodie, 2015; Jost et al., 2008; McGlothlin et al., 2014, 2016).

The interaction between toxic newts (*Taricha*) and resistant garter snake predators (*Thamnophis*) provides an ideal system for examining convergent evolution in an integrative framework. Pacific newts possess TTX (Brodie, 1968) they can excrete from the skin for defence (Cardall et al., 2004). *Thamnophis* from several populations in western North America are known to prey on sympatric newts with little to no ill effects (Brodie, 1968; Brodie & Brodie, 1990; Brodie et al., 2002; Brodie et al., 2005; Greene & Feldman, 2009; Wiseman & Pool, 2007). Furthermore, this ability to consume deadly newts appears to have evolved independently three or even four times within *Thamnophis* (Feldman et al., 2009; Hague et al., 2017).

Work on understanding this predatory adaptation has largely focused on the common garter snake (*Th. sirtalis*), which displays extensive geographical variation in TTX resistance across its range (Brodie & Brodie, 1990; Brodie & Brodie, 1991; Brodie et al., 2002; Hague et al., 2017) that roughly matches TTX levels in sympatric newt prey (Hanifin et al., 2008; Hague et al., 2020). Measures of whole-animal TTX resistance are tightly correlated to measures of resistance in isolated skeletal muscle (Geffeney et al., 2002), suggesting changes in muscle physiology underlie organismal resistance. The muscles, in turn, are resistant to TTX because specific P-loop replacements in the sodium channel expressed in skeletal muscle ($Na_v1.4$) reduce the ability of TTX to bind to this protein, allowing normal channel activity and thus muscle function (Geffeney et al., 2005). Indeed, point mutations in *SCN4A* in *Th. sirtalis* explain the majority of variation in TTX resistance measured at the whole-animal level (Feldman et al., 2010; Hague et al., 2017, 2020). This connection allows us to address questions about convergence at several biological levels: (i) whole animal; (ii) organ (muscle tissue); and (iii) protein, including: (a) structural changes (amino acid replacements) and (b) regulatory changes (expression levels).

The Sierra garter snake (*Th. couchii*) and three species of Pacific newts (*Taricha granulosa*, *Ta. sierrae*, *Ta. torosa*) that inhabit the Sierra Nevada Mountains and Cascade Ranges of California (Stebbins, 2003) are involved in a co-evolutionary arms race similar to the *Th. sirtalis* and *Ta. granulosa* system, with strong regional patterns of trait covariation across the shared range of these species (Reimche et al., 2020). TTX resistance varies several orders of magnitude within and among populations of *Th. couchii* (Reimche et al., 2020). Our goal is to determine if the same hierarchical mechanisms underpinning the predatory adaptation in *Th. sirtalis* are responsible for variation in TTX resistance in *Th. couchii*. We assess the extent of convergence between *Th. sirtalis* and *Th. couchii* by examining TTX resistance (and plausible resistance-conferring mechanisms) in *Th. couchii* at multiple levels: whole animal, muscle tissue, and genotype, including gene sequence and gene expression. First, we describe patterns of phenotypic TTX resistance in populations of *Th. couchii*. Second, we examine TTX resistance in skeletal muscle, as well as the correlation between variation in muscle and whole-animal TTX resistance. We then examine sequence variation in the three *SCN* genes (*SCN4A*, *SCN8A*, *SCN9A*) encoding the TTX-sensitive Na_v proteins that should be exposed to TTX during newt ingestion ($Na_v1.4$ in skeletal muscle, and $Na_v1.6$ and 1.7 in peripheral nerves, respectively). Functional variation in the P-loops of these loci are known to provide TTX resistance in other taxa (Jost et al., 2008; McGlothlin et al., 2016), and we expect allelic variation in the P-loops of these genes to correspond with whole-animal and muscle resistance. Lastly, we test whether differential expression of *SCN4A* (skeletal muscle sodium channel gene) is associated with TTX resistance in muscle tissue and at the whole-animal level. Changes in gene expression have not been explicitly addressed in this system but could provide an additional mechanism of TTX resistance (Feldman et al., 2016). Specifically, TTX resistance might be gained by increasing the expression of *SCN4A*, creating more $Na_v1.4$ in skeletal muscle than newt TTX can block. By examining the physiological and molecular underpinnings of TTX resistance in a parallel *Thamnophis* system, we hope to shed light on the predictability of convergent evolution across the levels of phenotypic organization.

2 | MATERIALS AND METHODS

2.1 | Field collections and captive care

We field-collected individual *Thamnophis couchii* from across the entire distribution of the species in the Sierra Nevada Mountains and Lower Cascade Ranges of California (Table S1). Our sample includes 293 snakes from 35 sites representing 12 distinct watersheds that we had previously examined (Brodie et al., 2005; Feldman et al., 2009; Reimche et al., 2020), plus 48 new samples from nine new sites and seven new watersheds, yielding a final data set of 341 *Th. couchii* from 44 unique sites and 19 distinct watersheds (Table S1).

Prior to phenotypic measures and physiological assays, we housed snakes individually in either 5- or 10-gallon tanks, depending on animal size. We provided each tank with a water dish, hide box (Reptile Basics), newspaper or sani-chip bedding (Harlan Teklad), full-spectrum lighting (Reptisun, 10.0 UVA/UVB; Exo Terra) and heat-tape placed under one end of the tank to generate a thermal gradient from roughly 24–30°C. We kept snakes in a room on a 12-hr:12-hr light–dark cycle with a constant temperature of 26°C and fed snakes either fish (live guppies or frozen trout) or feeder mice (frozen mice from a vendor) once or twice per week.

We followed protocols approved by the Utah State University (USU) and University of Nevada Reno (UNR) Institutional Animal Care and Use Committees (IACUC) for all care, handling and work on live snakes.

2.2 | Phenotype bioassays

2.2.1 | Whole-animal TTX resistance assay

We assessed the ability of live snakes to function under ecologically relevant amounts of TTX they might ingest. We used a well-established bioassay of whole-animal performance that compares the reduction in locomotor ability of individual snakes when subjected to increasing doses of TTX (Brodie & Brodie, 1990; Brodie et al., 2002; Ridenhour et al., 2004). Specific details of the whole-animal assay can be found in Brodie et al. (2002) and Ridenhour et al. (2004). Briefly, we placed snakes on a 3-m track lined with infrared sensors every 20 cm to record sprint speeds (as well as with a mounted video camera recording trials as a back-up). We used the mean of the quickest two interval times as a snake's speed. After measuring the baseline speed of each snake (pre-injection), we rested snakes for 48 hr and then gave each snake an intraperitoneal (IP) injection of TTX, starting at 1 mass-adjusted mouse unit (MAMU), where 1 MAMU is the amount of TTX needed to kill a 20-g mouse in 10 min, which corresponds to 0.01429 μg of TTX per gram of snake (Brodie & Brodie, 1990; Brown & Mosher, 1963; Ridenhour et al., 2004). We then recorded post-injection speeds 30 min after IP injection (Brodie et al., 2002; Ridenhour et al., 2004). We then repeated the process: after 48 h of rest, we injected snakes again with serially increasing doses of TTX (5, 10, 25, 50, 100 or 150 MAMUs), and recorded post-injection speeds. We scored resistance as the dose required to slow a snake to 50% of its pre-injection baseline speed (50% MAMU). We estimated this 50% dose using linear regression on log-transformed dosages (see Brodie et al., 2002; Reimche et al., 2020; Ridenhour et al., 2004).

2.2.2 | Skeletal muscle TTX resistance assay

In *Th. sirtalis*, whole-animal TTX resistance is tightly correlated with the ability of skeletal muscles to withstand TTX (Geffeney et al., 2002). To determine if *Th. couchii* and *Th. sirtalis* possess the same physiological mechanism of TTX resistance, we characterized skeletal muscle TTX resistance in *Th. couchii*. We collected muscle TTX resistance data from a subset of the same animals for which we obtained whole-animal TTX resistance data, sampling 25 *Th. couchii* from 10 localities spanning seven distinct watersheds to capture the geographical breadth and phenotypic variation seen across the range of the species. We subjected isolated muscle tissue to a dose–response protocol analogous to that of the whole-animal resistance assay, serially increasing doses of TTX to measure the concentrations of TTX that reduce muscle performance.

Following euthanasia, we immediately submerged snakes in physiological Krebs buffer perfused with 95% O_2/5% CO_2. We dissected and extracted 2–4 cm of the *iliocostalis* muscle (see Figure 2b), part of the dorsolateral muscle group involved in snake locomotion (Jayne, 1988). We then performed myography on a Contraction System Chamber 800A which we operated using the DYNAMIC MUSCLE CONTROL version 4 software (Aurora Scientific). Before suspending the muscle, we calibrated the force transducer with a 40-g load, well above the expected biological outputs. For all *Th. couchii*, we suspended the iliocostalis from the force transducer and secured it to the chamber platform by vessel clips or tied with nylon surgical sutures. We filled the chamber with the same Krebs buffer, continuously aerated with 95% O_2/5% CO_2 and maintained at 25°C. The entire length of the muscle was situated between equidistant parallel electric field stimulation (EFS) platinum electrodes. To optimize the protocol, we applied a 500-μs pulse of direct current in increasing magnitude from 1 to 300 mA under baseline tension of 0.1 g to suspend the muscle. The EFS stimulus was set to 1.5 times the smallest magnitude current that provided the greatest muscle contraction. At this optimum electrical stimulus, we optimized the length–tension relationship for each muscle by increasing the baseline tension until the force output peaked. We recorded all trials at 10-kHz sampling frequency.

We applied a pulse to induce muscle contraction at baseline (absence of TTX) and at serially increasing doses, allowing muscles 75 ± 15 s of rest between pulses. We added known doses of TTX in citrate buffer pH 6.8 to the bath of known volume. Doses began as low as 1 nM and increased until the transient force peak magnitude decayed. In many cases, we increased the concentration of TTX until the abolishment of muscular activity was achieved, though this was not possible for every experiment. We kept the volume of TTX in citrate buffer in the bath below 0.01% of the total bath volume to minimize effects of diluting the Krebs buffer and pH alterations. Note that we rested muscles for 75 ± 15 s between pulses, and preliminary trails showed that fatigue does not set in during this assay (muscles can maintain baseline force for several hours without TTX).

We generated dose–response curves from the peak transient contraction force magnitude and we fit responses to a sigmoidal curve described by the equation:

$$Force\left(Ng^{-1}\right) = A_2 + (A_1 - A_2) / (1 + e\{((\log([TTX](nM)) - \log(x_0)) / dx)) \quad (1)$$

where A_1 and A_2 are the upper- and lower-bounds, dx is the rate of decline in force with increasing [TTX], and x_0 is the centre of the curve (toxin concentration producing half-maximal inhibition, IC_{50}). We estimated this 50% concentration using the above sigmoidal fit on log-transformed dosages; concentrations equal to zero were set to 0.1. If the contraction recorded at 0 nM TTX was unusable, then we used the maximum force produced throughout the routine (frequently occurring within the first testing with 10 nM TTX).

We determined the relationship between whole-animal TTX resistance and skeletal muscle TTX resistance using simple linear regression and Spearman's rank correlation coefficient in R version 3.6.2 (R Core Team, 2019). We also compared the levels of TTX resistance at the whole-animal level between individuals from two populations (the Honey-Eagle Lakes watershed vs. Upper Tuolumne River Watershed), and compared levels of TTX resistance at muscle level between individuals from these populations using the nonparametric *t* test, Wilcoxon–Mann–Whitney test in R.

2.3 | Sodium channel sequencing

We examined sequence variation in the genes that encode three sodium channels that are normally sensitive to TTX: *SCN4A* (skeletal muscle sodium channel, $Na_V1.4$), *SCN8A* (motor neuron sodium channel, $Na_V1.6$) and *SCN9A* (sensory neuron sodium channel, $Na_V1.7$). We focused on DNA sequence variation in portions of the four domains (DI–DIV) that code for the P-loops of these voltage-gated sodium channels.

We extracted genomic DNA from tail-snips, skeletal muscle or liver tissue with the DNeasy Blood & Tissue Kit (Qiagen) and amplified fragments of genomic DNA corresponding to the four P-loops by PCR (polymerase chain reaction) using *Thamnophis*-specific primers (Table S2). We Sanger-sequenced fragments in both directions using amplification primers and used an ABI Prism 3730 DNA Analyser (Thermo Fisher Scientific) at the Nevada Genomics Center (University of Nevada, Reno, NV, USA) to resolve sequences. We edited raw chromatograms and aligned nucleotide sequences in GENEIOUS version 9.1.4 (Biomatters; Kearse et al., 2012) using a full *SCN4A* contig of *Th. couchii* (Feldman et al., 2009; GenBank FJ570812.1) and contigs of *SCN8A* and *SCN9A* from *Th. sirtalis* (McGlothlin et al., 2014; GenBank BK008864.1, BK008865.1). We then translated nucleotides to amino acid sequences in GENEIOUS to examine potential amino acid replacements in the P-loops. We aligned all *Th. couchii* sequences to reference sequences of *Th. sirtalis*, *Th. elegans* and the king cobra, *Ophiophagus hannah* (from McGlothlin et al., 2016; GenBank KJ908928.1, KJ908891.1, KJ908908.1, KJ908933.1, KJ908935.1, KJ908913.1, KJ908932.1, KJ908918.1, KJ908938.1, KJ908927.1, KX063605.1, KX079432.1, KX079373.1, KX079433.1, BK009416.1, BK009417.1, BK009418.1, BK009419.1). Our final data set included P-loop sequences of all four domains of *SCN4A* from 109 snakes from 23 localities, P-loop sequences of all four domains of *SCN8A* from 28 snakes from eight localities, and P-loop sequences of all four domains of *SCN9A* from 27 snakes from eight localities (Table 1), spanning the entire range of whole-animal and muscle TTX resistance. We submitted all sequences to GenBank (MT415671–MT415682, MT432928–MT433019, MT459158–MT459171, MT460471–MT460494; ON357429–ON357572).

Finally, we sought to identify other novel genetic changes (e.g., splice variation) that might provide TTX resistance by examining the entire coding region (CDS) of *SCN4A* from two *Th. couchii*. We compared sequences of the entire *SCN4A* from a highly resistant *Th. couchii* from Upper Tule River (Feldman et al., 2009; GenBank FJ570812.1) to that from a *Th. couchii* with low TTX resistance from Battle Creek. We isolated and purified mRNA from fresh skeletal muscle with the RNeasy Mini Plus Kit (Qiagen). We reverse transcribed total mRNA to cDNA with the iScript Select cDNA Synthesis Kit (BioRad) and oligo(dT) primers. We then amplified and sequenced a series of overlapping pieces of *SCN4A* to construct a complete contig of the locus using primers designed for *Thamnophis SCN4A* (Feldman et al., 2009). We edited raw reads and aligned sequences in GENEIOUS. We then translated the entire contig to amino acid sequences in GENEIOUS. We deposited this contig in GenBank (MT304461).

2.4 | Gene expression assay

In addition to examining structural variation in the Na_v proteins, we sought to quantify variation in the expression of *SCN4A* ($Na_v1.4$) using quantitative PCR (qPCR). Allelic variation at this locus predicts skeletal muscle resistance in *Th. sirtalis* (Geffeney et al., 2005) and explains a large proportion of whole-animal TTX resistance in *Th. sirtalis* (Feldman et al., 2010; Hague et al., 2017, 2020) and *Th. atratus* (Feldman et al., 2010). However, allelic variation in *SCN4A* cannot entirely explain variation in TTX resistance, and the remaining phenotypic variation may be correlated with changes in the level of expression of *SCN4A*. We therefore expected increased levels of *SCN4A* expression in *Th. couchii* with high TTX resistance compared to those with low resistance.

2.4.1 | Tissue collection

We dissected a segment of skeletal muscle (*iliocostalis*) immediately following euthanasia. We stored all tissue samples in RNA*later* (Thermo Fisher Scientific) at −80°C. We collected tissues from 23 *Th. couchii* from eight localities with varying levels of TTX resistance: 10 individuals with low TTX resistance (≤5 MAMU) from the Battle Creek and Honey-Eagle Lakes watersheds, and 13 individuals with high TTX resistance (20–140 MAMU) from the Upper Tuolumne River, Upper Kings River and Upper Tule River watersheds. We extracted RNA from snake skeletal muscle tissue using the same protocol above with the exception of an additional cDNA conversion step; we used both SuperScript III reverse transcriptase (Invitrogen, Thermo Fisher Scientific) and random hexamers, and iScript Select cDNA Synthesis kit (BioRad) with oligo (dT) primers.

2.4.2 | Quantitative polymerase chain reaction

To measure gene expression profiles in *SCN4A*, we conducted qPCR in two different laboratories and with two different approaches to verify robustness of the results. For both experiments, we amplified a fragment of *SCN4A* corresponding to a P-loop region (Table S3) and normalized *SCN4A* expression means to a housekeeping gene, 18S ribosomal RNA (*18S*), known to have even expression patterns across tissue types and species of vertebrates (Currier et al., 2012; Vandesompele et al., 2002). For samples collected from the Honey-Eagle Lakes and Upper Tuolumne River watersheds, we performed qPCR in triplicate on all cDNA samples using custom designed TaqMan gene expression assays and mastermix (Applied Biosystems) on an ABI 2720 real-time thermocycler according to the recommended cycling parameters. We also normalized *SCN4A* expression means to an additional housekeeping gene, glyceraldehyde

TABLE 1 Major watershed (source) ordered from north to south, with mean phenotypic measures, standard deviation (*SD*) and sample sizes (*n*), as well as genotypes for *Thamnophis couchii* populations sampled for whole-animal TTX resistance, muscle physiology, sodium channel sequencing (*SCNA* loci) and qPCR work (*SCN4A*). Mean whole-animal TTX resistance is given as intraperitoneal injections (IP) of MAMUs (mass adjusted mouse units) of TTX required to reduce a snake to 50% of its baseline performance speed, to allow direct comparison to prior work on *Thamnophis* using those measures (e.g., Brodie et al., 2002). P-loop mutations that define the *SCNA* alleles are provided and shown in Figure 3. *SCN4A* expression levels are reported as fold change relative to the housekeeping gene (*18S*)

Watershed	$\bar{x}$ whole-animal TTX resistance & *SD*; 50% MAMU TTX (*n*)	$\bar{x}$ skeletal muscle TTX resistance & *SD*; IC_{50} nM TTX (*n*)	*SCN4A* allele (*n*)	*SCN8A* allele (*n*)	*SCN9A* allele (*n*)	*SCN4A* copy number; expression relative to *18S* (*n*)
1. Lower Pit River	1.70, 0.37 (4)	–	–	–	–	–
2. Battle Creek	2.58, 0.70 (13)	–	T (8)	V (4)	ENGY (3)	19.51 (2)
3. Honey-Eagle Lakes	4.41, 2.17 (28)	197.13, 172.26 (8)	T (18)	V (7)	–	8.63 (8)
4. Thomes Creek	1.32, N/A (1)	–	–	–	–	–
5. North Fork Feather River	18.27, 4.75 (5)	–	–	–	–	–
6. Middle Fork Feather River	1.10, N/A (1)	–	T (1)	–	–	–
7. Upper Yuba River	14.56, 17.13 (60)	115.43, 168.78 (4)	T (32)	–	–	–
8. South Fork American River	52.54, 32.97 (11)	–	–	–	–	–
9. Upper Carson River	17.40, N/A (1)	–	–	–	–	–
10. Upper Cosumnes River	54.20, 24.12 (50)	–	T (12)	–	–	–
11. Upper Mokelumne River	18.43, 17.36 (11)	321.32, N/A (1)	T (1)	–	–	–
12. West Walker River	3.10, N/A (1)	430.65, N/A (1)	T (1)	–	–	–
13. Upper Stanislaus River	15.70, 17.56 (2)	–	T (2)	–	–	–
14. Upper Tuolumne River	52.15, 39.01 (20)	1497.14, 718.70 (9)	T (18)	V (8)	EGNY (8)	8.83 (7)
15. Upper San Joaquin River	3.10, N/A (1)	197.40, N/A (1)	–	–	–	–
16. Upper Kings River	100.74, 22.76 (20)	–	T (10)	–	–	32.95 (4)
17. Tulare Lake Bed	40.74, N/A (1)	366.12, N/A (1)	–	–	–	–
18. Upper Tule River	87.26, 24.93 (107)	–	T (6)	V (8)	EGNY (5)	3.01 (2)
19. Upper Deer Creek	130.00, 34.68 (4)	–	T (2)–	–	–	–

Abbreviation: N/A, not applicable.

3-phosphate dehydrogenase (*GAPDH*). For samples collected from the Battle Creek, Upper Kings River and Upper Tule River watersheds, we performed qPCR in duplicate on all cDNA samples using the SYBR green chemistry assay (Applied Biosystems) on an MJ-Research Chromo 4 real-time thermocycler (BioRad) according to the recommended cycling parameters.

We determined relative gene expression using the comparative CT method (ΔΔCt) detailed in the ABI Guide to Performing Relative Quantitation of Gene Expression using Real-Time Quantitative PCR (Applied Biosystems, 2008). We used the average value from triplicate and duplicate runs for analysis. To account for batch effects among our two data sets, we applied a nonparametric empirical Bayes framework that adjusts normalized CT values using the ComBat function in the *sva* package in R (Johnson et al., 2007; Leek et al., 2012). Using the combined data, we normalized *SCN4A* ($Na_v1.4$) to *18S* and a control snake (a *Th. sirtalis*). Data were not normally distributed, so we compared relative expression among low- and high-resistance individuals using a nonparametric *t* test, Wilcoxon–Mann–Whitney test in R. We also performed linear regressions of relative expression levels against whole animal TTX resistance (50% MAMU) and muscle tissue resistance (IC_{50}).

3 | RESULTS

3.1 | Phenotype bioassays

3.1.1 | Whole-animal TTX resistance

The addition of new animals (n = 48) from several new watersheds provides a comprehensive geographical sample of snakes (n = 341), strengthening the overall patterns revealed by Reimche et al. (2020) of extensive variation in TTX resistance across the range of *Thamnophis couchii* (Figure 1; Table 1). These geographical patterns in whole-animal resistance are discussed at length in Reimche et al. (2020). Briefly, populations of *Th. couchii* exhibit clinal phenotypic variation, from low TTX resistance in the north to extreme TTX resistance in the south. Northern populations contain snakes with resistance as low as 1–2 MAMUs, while southern populations include snakes that can maintain sprint performance at doses exceeding 100 MAMU (i.e., snakes can function at mass-adjusted doses of TTX that would kill over 100 mice). These highly resistant *Th. couchii* possess phenotypes that exceed the TTX resistance of Oregon *Thamnophis sirtalis* (Brodie et al., 2002; Hague et al., 2017) but are roughly an order of magnitude lower than the most TTX-resistant *Th. sirtalis* (Brodie et al., 2002; Hague et al., 2017) and *Th. atratus* (Feldman et al., 2010) from central California. Among-population variation in *Th. couchii* is comparable to that observed in *Th. sirtalis* (Brodie et al., 2002; Hague et al., 2017). However, within-population variation in resistance in *Th. couchii* is considerable, especially in the central Sierra Nevada, where the snakes within some watersheds showed a tremendous range in phenotypes, such as 10–100 MAMU, ($\bar{x}$ = 54.20, SD = 24.12) in the Upper Cosumnes River, 6–100 MAMU ($\bar{x}$ = 52.54, SD = 32.97) in South Fork American River and 3–135 MAMU ($\bar{x}$ = 52.15, SD = 39.01) in Upper Tuolumne River watersheds (Table 1). This degree of phenotypic variation within sites has only been observed in a few other garter snake populations (Brodie et al., 2002; Feldman et al., 2010; Hague et al., 2017).

3.1.2 | Skeletal muscle TTX resistance

Myography assays from a subset of *Th. couchii* (n = 25) from seven watersheds also shows broad variation in skeletal muscle TTX resistance (Table 1). Individual TTX resistance (IC_{50}) ranged from 16 to 2400 nM TTX. Northern and southern populations of *Th. couchii* display significantly different resistance levels (Wilcoxon rank sum test W = 1, p < .001; see Figure 4); muscles from *Th. couchii* of the Honey-Eagle Lakes watershed in Lassen County have mean TTX resistance levels of 200 nM TTX (max = 540 nM TTX), while muscles from snakes of the Upper Tuolumne River watershed in Tuolumne County have mean TTX resistance levels of 1500 nM (min = 450 nM). These numbers are comparable to TTX resistance in the skeletal muscles of *Th. sirtalis*. However, as with whole-animal measures, the most resistant muscles from *Th. sirtalis* are an order of magnitude higher than those seen in *Th. couchii*, with muscles from some central California *Th. sirtalis* displaying IC_{50} values as high as 42,000 nM TTX (Geffeney et al., 2002). As in *Th. sirtalis* (Geffeney et al., 2002), whole-animal TTX resistance (50% MAMU) and skeletal muscle TTX resistance (IC_{50}) are highly correlated (Spearman's rank correlation; r = .71, R^2 = .72, F_{24} = 59.93, p < .001). In general, skeletal muscle TTX resistance predicts whole-animal TTX resistance and is responsible for a large proportion of the variation in whole-animal resistance (Figure 2).

3.2 | Sodium channel sequences

Sequence data reveal that the three TTX-sensitive sodium channels of *Th. couchii* contain resistance-conferring mutations in the pore-forming segments (P-loops) that interact with TTX. However, each channel paralogue is fixed for a single resistance-conferring allele across the entire species. Thus, functional sequence variation in sodium channels appears to be lacking at the individual and population levels. First, all *Th. couchii* contain the same mutation in the skeletal muscle channel gene, *SCN4A* (encoding $Na_v1.4$): a single amino acid substitution (M1267T) in the DIII P-loop of $Na_v1.4$ at a critical TTX binding site (detailed in Feldman et al., 2009) (Figure 3; Table 1). This mutation appears to be unique among snakes (Feldman et al., 2012; McGlothlin et al., 2016), but is seen in several other TTX-resistant taxa (Geffeney et al., 2019; Gendreau et al., 2021; Jost et al., 2008; Vaelli et al., 2020; Vlasenko et al., 2021) and confers a roughly 15-fold reduction in TTX ligation to the pore (Jost et al., 2008). Additionally, we found that all *Th. couchii* are fixed for ancestral P-loop substitutions in the motor nerve channel gene *SCN8A* ($Na_v1.6$) and sensory nerve channel gene *SCN9A* ($Na_v1.7$)

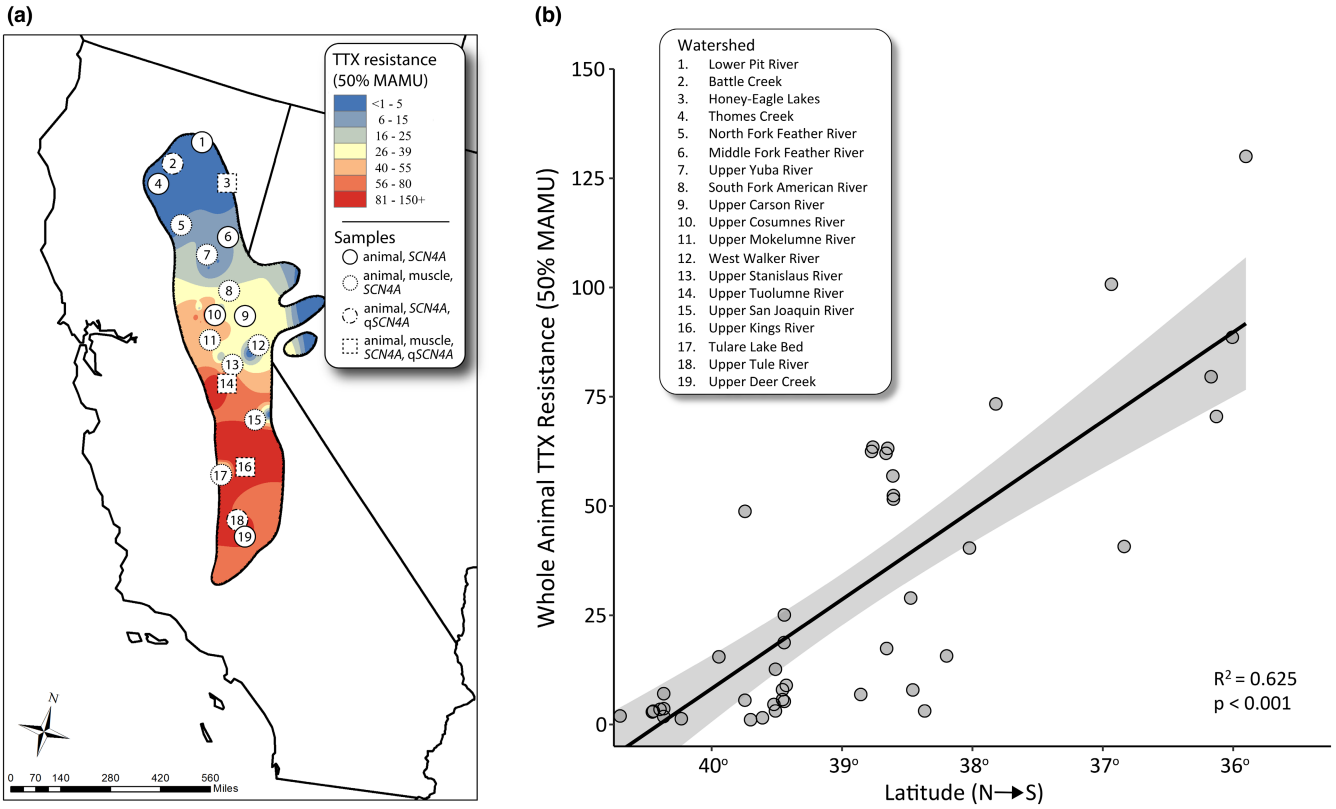

FIGURE 1 Geographical distribution of TTX resistance phenotypes for the Sierra garter snake (*Thamnophis couchii*) in California, and latitudinal gradient in phenotypes. (a) Map of whole-animal TTX resistance, scored as the amount of TTX required to slow a snake to 50% of its baseline speed, given in mass-adjusted mouse units (50% MAMU). Distribution of phenotypes based on interpolation of over 340 samples from 44 localities, sampled across 19 different watersheds in the Sierra Nevada and Cascade Ranges. Symbols denote the type of data collected from animals from the 19 watersheds: circles: whole-animal TTX phenotypes and DNA sequences from the skeletal muscle sodium channel gene (*SCN4A*); dashed circle: whole-animal TTX resistance, skeletal muscle TTX resistance and *SCN4A* sequences; long–short dashed circle: whole-animal TTX resistance, *SCN4A* sequences and relative *SCN4A* expression data (q*SCN4A*); dashed square: whole-animal TTX resistance, skeletal muscle TTX resistance, *SCN4A* sequences, *SCN8A* sequences (motor neuron sodium channel gene), *SCN9A* sequences (sensory neuron sodium channel gene) and q*SCN4A*. (b) Linear relationship between TTX resistance and latitude ($r = .79$, $R^2 = .62$, $F_{1,330} = 39.17$, $p < .001$); based on mean TTX resistance (50% MAMU) of animals from 44 sites. Whole-animal data from Brodie et al. (2005), Feldman et al. (2009), Reimche et al. (2020) and this study; map modified from Reimche et al. (2020) [Colour figure can be viewed at wileyonlinelibrary.com]

(Figure 3; Table 1). In *SCN8A*, there is a single amino acid substitution in the DIV P-loop (I1709V) which is ancestral in New World natricine snakes (including *Thamnophis*) and appears in a few other advanced snake families (McGlothlin et al., 2016). In *SCN9A*, there are four P-loop substitutions, one in DIII (D1393E) and three in DIV (A1681G, D1684N, G1685Y). These same *SCN9A* P-loop substitutions are seen across the phylogeny of advanced snakes (including *Thamnophis*), including both TTX-resistant and TTX-sensitive snakes (McGlothlin et al., 2016).

We found just a single amino acid difference (G984W) in the full CDS of *SCN4A* between high TTX-resistant (Upper Tule River watershed) and low TTX-resistant *Th. couchii* (Battle Creek watershed). This G984W replacement was found in the Battle Creek population and appears uniquely derived, as other *Thamnophis* and even *Homo* possess the ancestral G at this position. However, this substitution occurs in the intracellular region between the second and third domain of the P-loop and is not likely to influence TTX resistance (Fozzard & Lipkind, 2010).

3.3 | Sodium channel gene expression

Using qPCR, we were able to identify the presence and quantity of both housekeeping genes (*GAPDH* and *18S*) and the gene of interest (*SCN4A*) in muscle tissue. When we compared the expression of *SCN4A* by phenotype, we found no significant differences in mean relative gene expression (Figure 4; Table S4). Relative to *18S*, TTX-resistant snakes expressed *SCN4A* with a 15-fold increase (±14.5) compared to a 10-fold increase (±9.9) in snakes with low TTX resistance. Relative to *GAPDH*, TTX-resistant snakes expressed *SCN4A* with a 4-fold increase (±4.5) compared to a 2-fold increase (±2.0) in those with low TTX resistance. While this trend is interesting, variance in each group was large, and statistical analyses indicate no significant differences in relative gene expression of *SCN4A* between TTX-resistant and TTX-sensitive snakes, as normalized to our housekeeping genes (*18S*: Wilcoxon rank sum test $W = 23$, $p = .38$; *GAPDH* $W = 27$, $p = .65$). Additionally, there was no linear relationship between relative expression of *SCN4A*

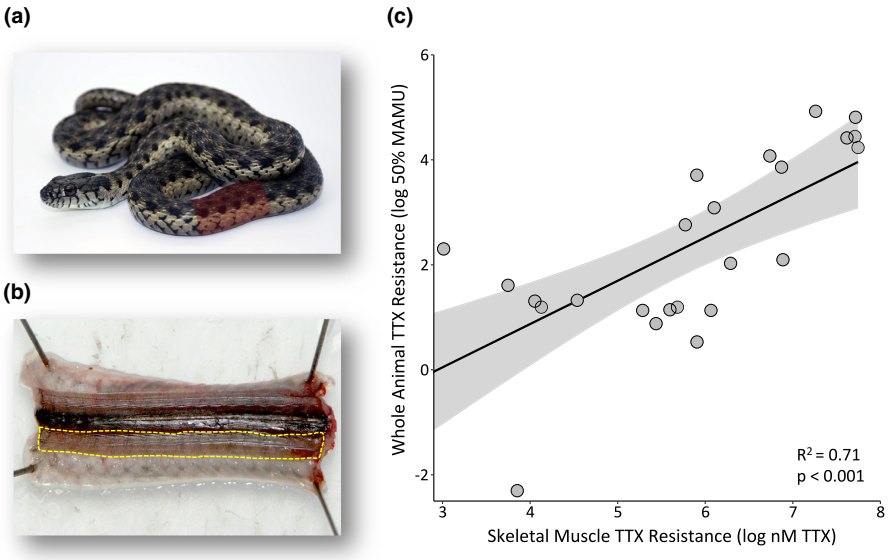

FIGURE 2 Quantification of TTX resistance in skeletal muscles and relationship between tissue and organismal resistance. (a) *Thamnophis couchii* showing the dorsal region (red area) used for myography. (b) Pinned section of snake (dorsal view), with skin removed, revealing the *iliocostalis* muscle (dashed outline) isolated, dissected and then suspended from a force transducer to measure contractile force and skeletal muscle TTX resistance. (c) Linear relationship between whole-animal TTX resistance and skeletal muscle TTX resistance in *Th. couchii* sampled from multiple sites across seven watersheds. Whole-animal TTX resistance is reported as the amount of TTX required to slow a snake to 50% of its baseline speed, in mass-adjusted mouse units (50% MAMU). Skeletal muscle resistance was measured as the concentration of TTX required to reduce a skeletal muscle to 50% its original contraction force (IC_{50}; 50% inhibition concentration). Skeletal muscle phenotypes strongly predict whole-animal phenotypes ($r = .71$, $R^2 = .72$, $F_{1,24} = 59.93$, $p < .001$). Figure shown on log scale for ease of viewing, but regression performed on raw (untransformed) data. Photo credit: D. A. Picklum [Colour figure can be viewed at wileyonlinelibrary.com]

and whole-animal phenotype (50% MAMU: Spearman's rank correlation; $r = .06$, $R^2 = .01$, $F = 1.22$, $p = .28$) or skeletal muscle phenotype (IC_{50}: Spearman's rank correlation; $r = -.05$, $R^2 = .01$, $F = 0.12$, $p = .73$) (Figure S1).

4 | DISCUSSION

Here, we examine toxin resistance across levels of biological organization in the Sierra garter snake (*Thamnophis couchii*) to explore the degree of convergent evolution between this species and the common garter snake model (*Th. sirtalis*). We find convergence in the whole-animal phenotype and the organ level, suggesting similar physiological mechanisms of resistance, but simultaneously find a mix of consistency at the molecular level of protein structure and regulation (Table 2). These results suggest that selection shapes the outward-most facing phenotypes, but that different lineages can accomplish similar physiological adaptations through alternative molecular mechanisms.

4.1 | Levels of convergence in TTX resistance

The Sierra garter snake (*Th. couchii*) demonstrates wide variation in whole-animal TTX resistance (Figure 1), generally matching TTX levels in their sympatric newt prey (Reimche et al., 2020), similar to the geographical structure of arms-race matching seen between the common garter snake (*Th. sirtalis*) and its prey (Hanifin et al., 2008; Hague et al., 2020). Variation in whole-animal TTX resistance in *Th. couchii* is largely predicted by variation in TTX resistance in muscle (Figure 2), as observed in *Th. sirtalis* (Geffeney et al., 2002). These results suggest that TTX resistance in skeletal muscle is the primary physiological mechanism underlying this predatory adaptation in both *Th. couchii* and *Th. sirtalis*. If *Th. atratus* (a third species of garter snake known to be TTX-resistant; Feldman et al., 2009, 2010) also shows the same correlation between whole-animal and muscle resistance, then all three TTX-resistant garter snake species have converged on the same physiological path of toxin resistance.

The molecular underpinning of TTX resistance is thought to be functional variation in the P-loops of voltage-gated sodium channels (Na_v loci), which show convergent replacements across the many species of metazoans that have evolved TTX resistance (e.g., Feldman et al., 2012; Geffeney et al., 2019; Gendreau et al., 2021; Jost et al., 2008; Vlasenko et al., 2021). We first screened variation in *SCN4A*, the gene that encodes the sodium channel expressed in skeletal muscle ($Na_v1.4$), as variation at this locus appears to explain whole-animal phenotypes in *Th. sirtalis* (Feldman et al., 2010; Geffeney et al., 2005; Hague et al., 2017, 2020). Indeed, *SCN4A* in *Th. couchii* contains a mutation (M1267T) at a critical residue in the DIII P-loop (Feldman et al., 2009) shown to be under positive selection in newts (Gendreau et al., 2021) and modelled to interact with TTX (Tikhonov & Zhorov, 2005, 2011). Substitutions at this site alter TTX ligation to the outer pore of the channel (Terlau et al., 1991; Du et al., 2009), and when this exact mutation was constructed in rat $Na_v1.4$, it led to a 15-fold increase in TTX resistance (Jost et al., 2008). This same replacement has evolved

multiple times in TTX-resistant taxa, including Pacific newts (Hanifin & Gilly, 2015; Vaelli et al., 2020; Gendreau et al., 2021), pufferfishes (Jost et al., 2008), and even invertebrates such as blue-ringed octopus (Geffeney et al., 2019) and some marine ribbon worms (Vlasenko et al., 2021). Oddly, however, large differences in TTX resistance at both the whole-animal and muscle level in *Th. couchii* are not explained by allelic differences in *SCN4A*, as all our snakes possess this same M1267T substitution observed elsewhere to confer TTX resistance (Jost et al., 2008).

We then screened variation in two other candidate genes (*SCN8A* and *SCN9A*) that encode TTX-sensitive sodium channels ($Na_v1.6$ and $Na_v1.7$) known to contain TTX-resistant replacements in *Th. sirtalis* and other snakes (McGlothlin et al., 2014, 2016), as well as in their equivalent paralogues in newts (Vaelli et al., 2020; Gendreau et al., 2021) and pufferfish (Jost et al., 2008). Again, *Th. couchii* display resistance-conferring mutations in their sodium channels, but no amino acid sequence variation in these paralogues. In fact, all *Th. couchii* individuals possess the same resistance-conferring mutations in *SCN8A* and *SCN9A* seen in *Th. sirtalis* (McGlothlin et al., 2014). The *SCN8A* and *SCN9A* P-loop replacements shared by *Th. couchii* and *Th. sirtalis* are ancient mutations that evolved long before the genus *Thamnophis* (McGlothlin et al., 2016), some of which are hypothesized to have originated in the common ancestor of squamate reptiles (McGlothlin et al., 2016). Thus, all *Th. couchii* appear fixed for the same ancestral replacements in the sodium channels of peripheral nerves that appear to provide low levels of TTX resistance in colubrid snakes (McGlothlin et al., 2016).

Because structural differences (amino acid replacements) in the *SCN* genes do not explain variation in phenotypic resistance, we explored whether patterns of *SCN* gene expression might be correlated with phenotypic variation. Differential gene expression of members of the *SCN* gene family could provide an alternate or additional source of variation in TTX resistance (Feldman et al., 2016), as up-regulation of certain *SCN* genes may increase production of resistant channels in the skeletal muscle and nerve tissue affected by TTX. However, we found no significant differences in the relative expression of *SCN4A* in skeletal muscle among populations representing extremes of TTX resistance (Figure 4). Additionally, we found no relationship between relative *SCN4A* expression and whole-animal TTX resistance or muscle resistance (Figure S1). Though mRNA expression and protein expression are generally correlated, actual levels of Na_v expression should still be quantified. It remains to be seen whether other *Thamnophis* species express *SCN4A* (and $Na_v1.4$) at similar levels, and whether changes in expression might provide some measure of TTX resistance in snakes. It may be that up-regulation of *SCN4A* is a plastic response to intoxication, and occurs immediately upon exposure to TTX.

4.2 | Alternative routes to TTX resistance

To our knowledge, there are only a few other cases where animals exhibit variation in TTX resistance at the whole-animal level without associated variation in the P-loops of TTX-sensitive sodium channels. In the model *Th. sirtalis* system, there are snakes in certain populations (e.g., Monterey Co. CA, Sonoma Co. CA, Giles Co. VA) that exhibit modest levels of resistance, yet those phenotypes are not accompanied by P-loop variation in *SCN4A* (Feldman et al., 2009, 2010; Hague et al., 2017). A more extreme case is found in the eastern hog-nosed snake (*Heterodon platirhinos*), where several populations display high levels of TTX resistance but possess the same ancestral *SCN4A* allele found in all TTX-sensitive snakes (Feldman et al., 2016). The situation with *Th. couchii* is perhaps odder still—the species shows extensive variation in whole-animal TTX resistance and correlated muscle resistance, despite the fact that all populations are fixed for the same *SCN4A* mutation (M1267T) known to confer resistance on other genetic backgrounds (Jost et al., 2008). If all snakes have the same resistance-conferring mutation in their skeletal muscle, then how are some animals (and their muscles) so sensitive to low levels of TTX and others so resistant?

Multiple hypotheses could explain TTX resistance in the absence of allelic variation in *SCN4A* or differences in the expression of *SCN4A*. The first involves changes in the expression of other candidate genes. While we did not observe significant differences in gene expression of our single candidate gene, *SCN4A*, TTX resistance may still be at least partly conferred by differential gene expression of other targets of TTX, loci of the *SCN* gene family ($Na_v1.1$–$Na_v1.9$). In mammals, multiple Na_v paralogues are expressed in early development (Rogart et al., 1989; Stocksley et al., 2005) and different Na_v paralogues have even been isolated from skeletal muscle and cardiac tissue (Krause et al., 2015; Maier et al., 2004; Rogart et al., 1989; Stocksley et al., 2005). If reptiles display similar expression profiles as they develop, then simple adjustments that continue the expression of TTX-insensitive channels (e.g., Na_v 1.5, $Na_v1.8$ and Na_v 1.9) in muscle tissue as snakes age could contribute to muscle resistance. Therefore, differential expression of TTX-sensitive and TTX-insensitive Na_v paralogues could be a causal factor in the variation in underlying resistant phenotypes (Feldman et al., 2016; Huey & Moody, 2002). Even differences in translation or degradation of Na_v channels might contribute to phenotypic variation.

There may also be novel genes and regulatory regions involved in the production of TTX-resistant phenotypes. To date, work on understanding the genetic basis of TTX resistance in *Thamnophis* has centred on functional variation in the α-subunits of Na_v proteins (Feldman et al., 2009, 2010, 2012; Geffeney et al., 2005; Hague et al., 2017, 2020; McGlothlin et al., 2014, 2016; Perry et al., 2018). These large subunits create the membrane spanning channel and the outer pore that is the target of TTX. However, each Na_v α-subunit possesses one or two accessory β-subunits that are responsible for modulating channel gating, regulating channel expression in the cell membrane, and controlling neuron excitability (Isom, 2001; Namadurai et al., 2015). It seems plausible that variation in the β-subunits on TTX-targeted channels could contribute to resistance by altering the density of channel expression in certain tissues (Chen et al., 2002; Lopez-Santiago et al., 2006). An increased density of sodium channels in the membrane at the neuromuscular junction and throughout the sarcolemma could serve as a buffer against TTX blockade, because essentially doubling the abundance of sodium channels in the membrane should leave a reserve of channels large

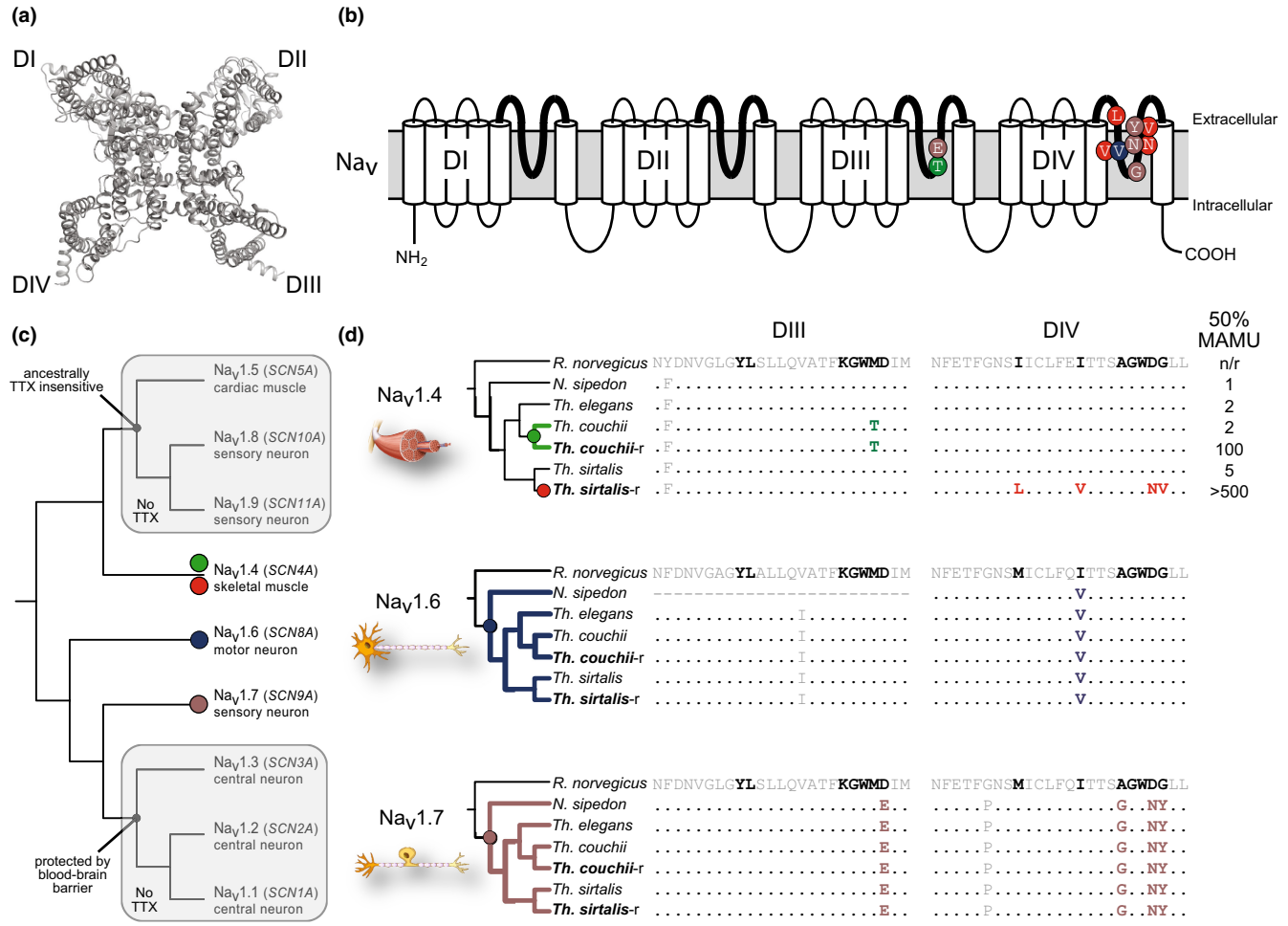

FIGURE 3 Evolutionary genetics of TTX resistance in two species of *Thamnophis*. (a) Structural model of the α-subunit of voltage-gated sodium channel (Na_v protein) (model courtesy of K. Stanek). Top-down view, showing all four domains (DI–DIV) that fold together to form a membrane-spanning channel; the outer pore of the channel (central opening) is created by four peptide chains (P-loops) that allow selective permeation of Na^+ but also form the binding sites for TTX. (b) 2D cartoon of Na_v protein highlighting the P-loops (bold) that form the outer pore (modified from Feldman et al., 2009). Specific mutations in the DIII and DIV P-loops confer TTX resistance to each paralogue: $Na_v1.4$ (green and red), $Na_v1.6$ (dark blue) $Na_v1.7$ (purple). (c) Amniotes possess nine functional sodium channel paralogues, each expressed in specific organs and each encoded by a single *SCN* gene (Na_v phylogeny after Zakon et al., 2011). However, three of these are ancestrally insensitive to TTX because of critical replacements in the DI P-loop, and three others are sheltered from TTX by the blood–brain barrier (grey boxes). Thus, TTX resistance in *Thamnophis* is expected to occur through convergent changes in the remaining TTX-sensitive channels (mutations indicated by coloured circles). (d) Amino acid sequences of DIII and DIV P-loops of TTX-sensitive Na_v from *Homo*, an outgroup natricine snake (*Nerodia sipedon*) and three *Thamnophis* species, including representatives from the most and least TTX-resistant *Th. couchii* populations, and *Th. sirtalis* from Willow Creek displaying dramatic variation in TTX resistance (50% MAMU shown; n/r = nonresistant). P-loop residues known to interact with TTX are dark, and coloured residues indicate TTX-resistant mutations. Mutations have been mapped onto the phylogeny of representative animals that display where on the tree TTX-resistant mutations arose. Note mutations in $Na_v1.6$ and $Na_v1.7$ pre-date garter snakes, and appear to give some clades of advanced snakes some base level of TTX resistance, and independent mutations then arise in $Na_v1.4$ in *Th. sirtalis* and *Th. couchii* (see McGlothlin et al., 2016). However, we also note that variation in TTX-resistance-conferring mutations in $Na_v1.4$ correspond to variation in TTX resistance in *Th. sirtalis* but not *Th. couchii*. Phenotypic data from Feldman et al. (2009) and this study; sequence data from McGlothlin et al. (2016), Perry et al. (2018) and this study [Colour figure can be viewed at wileyonlinelibrary.com]

enough to maintain motility in the face of a TTX challenge. However, due to the threshold nature of sodium channels, a membrane density of channels sufficient to defend against TTX intoxication might provide more opportunities to generate errant or ectopic action potentials, in turn making the muscles prone to hyperexcitability. Moreover, routine tests of muscle activity showed no indication *Th. couchii* muscles are hyperexcitable in the absence of TTX (data not shown).

Third, there may be other resistance-conferring mechanisms that do not involve changes to sodium channels. One plausible hypothesis involves the presence of a TTX binding glycoprotein in the blood plasma, as seen in various pufferfish species (Matsui et al., 2000; Yotsu-Yamashita et al., 2010; Yotsu-Yamashita et al., 2018). Recent work on toxin resistance in batrachotoxin-bearing frogs and birds also hints at the role of toxin scavenging proteins that can sequester sodium channel blockers and protect animals from their own poisons (Abderemane-Ali

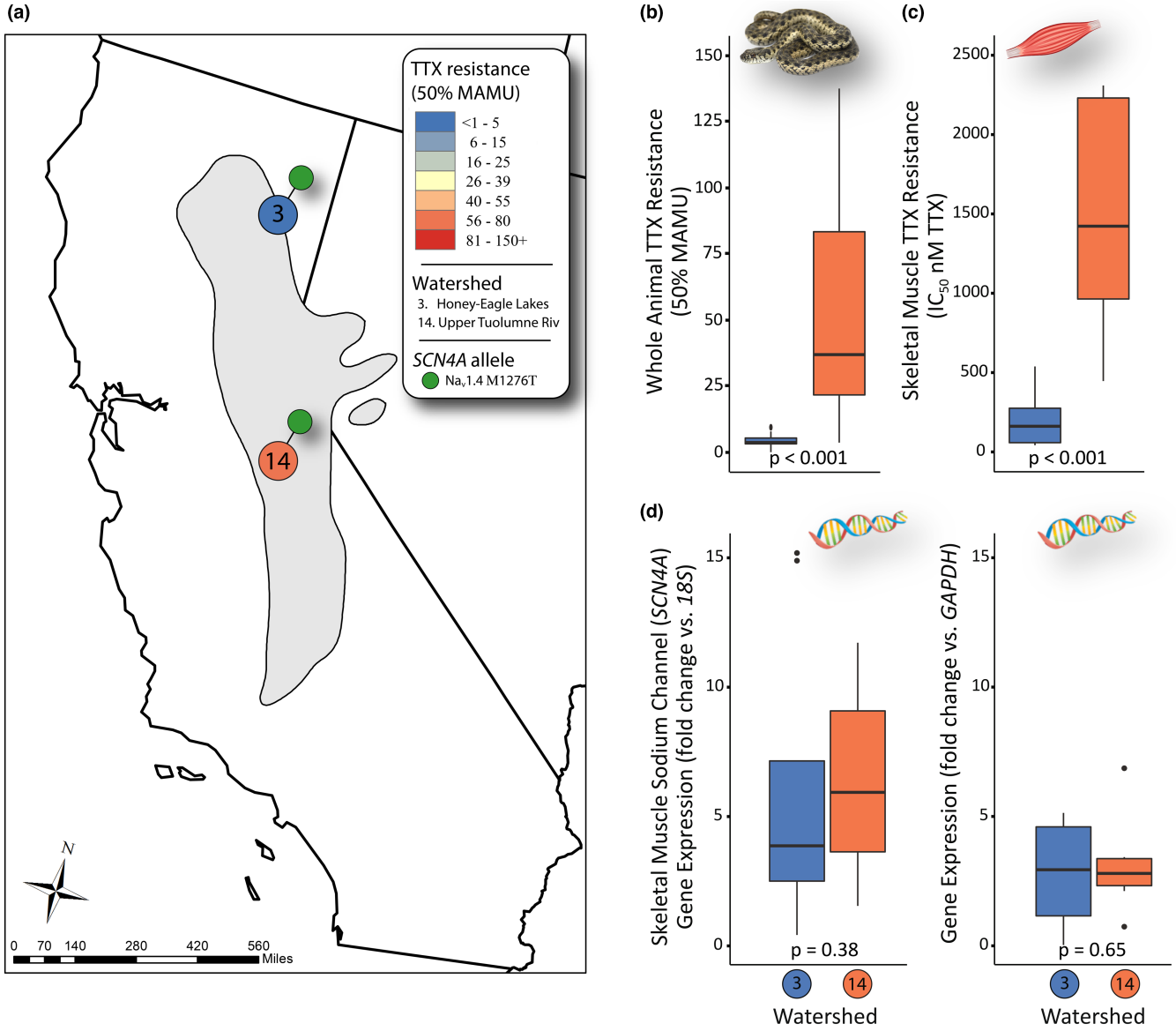

FIGURE 4 Geographical distribution of TTX resistance (phenotypes) and sodium channel alleles (genotypes), along with comparisons of TTX resistance at three different biological scales in two populations. (a) Range of *Thamnophis couchii* showing mean whole-animal TTX resistance (50% MAMU) for sampled watersheds (numbered circles), as well as the frequency of the skeletal muscle sodium channel allele (*SCN4A*) observed in populations (green circles). Note that each population is fixed for a single allele (M1267T), despite variation in whole-animal and muscle phenotypes within and among populations. (b) Organismal TTX resistance, measured as the amount of TTX required to slow a snake to 50% of its normal crawl speed (50% MAMU), is significantly different between northern (Honey-Eagle Lakes watershed: blue) and southern (Upper Tuolumne River watershed: orange) populations (Wilcoxon rank sum test, $W = 43$, $p < .001$). (c) Skeletal muscle TTX resistance, in dose of TTX (nM) required to reduce muscles to 50% of normal contraction (IC_{50}), also shows a significant difference across populations ($W = 1$, $p < .001$). (d) However, there are no differences in the expression of *SCN4A*, encoding skeletal muscle sodium channels ($Na_v1.4$), using two different housekeeping markers as controls (*18S*: $W = 23$, $p = .38$; *GAPDH*: $W = 27$, $p = .65$) [Colour figure can be viewed at wileyonlinelibrary.com]

et al., 2021; Tarvin et al., 2016). Another possible mechanism involves barriers to the diffusion of TTX across the gut, as postulated in some insects and crustaceans (Wilson et al., 2014; Mebs et al., 2016).

Lastly, it may be important to consider the phylogenetic and biogeographical history of *Th. couchii* to understand the evolution of TTX resistance in this taxon. Because M1267T appears fixed across populations of *Th. couchii*, this mutation is probably ancestral. This would suggest that M1267T, and by extension TTX resistance, evolved early in the history of *Th. couchii*. However, potential costs to TTX resistance (Brodie & Brodie, 1999; Feldman et al., 2012; Hague et al., 2018) may have led to the subsequent reduction and even loss of TTX resistance in northern populations. Rather than lose M1267T altogether, some other mechanism may have led to a reduction and loss of TTX resistance in muscles and at the whole-animal level (apparently not involving regulatory or amino acid changes in *SCN4A* in muscle). In other words, did elevated TTX resistance in *Th. couchii* evolve in parallel to other systems, but subsequent TTX sensitivity evolve a different way? Determining the phylogeographical history

TABLE 2 Summary of the degree of convergent evolution in adaptive TTX resistance in two garter snake species, *Thamnophis sirtalis* (common garter snake) and *Th. couchii* (Sierra garter snake). Similarity between these species occurs across levels of biological organization, from higher-order phenomena (top) to lower-level mechanisms (bottom). Because these snakes are distantly related (Hallas et al., 2022), and intervening snakes along the phylogeny do not exhibit most of these derived traits (e.g., Feldman et al., 2009; McGlothlin et al., 2016), we can infer the evolutionary pathway of resistance as occurring by convergence (green), divergence (red), common ancestry (grey) or still unknown (yellow) [Colour Table can be viewed at wileyonlinelibrary.com]

Scale of Pattern or Mechanism (TTX resistance)	Common garter snake *Th. sirtalis*	Sierra garter snake *Th. couchii*	Evolutionary Pathway
Ecological Interaction (snakes prey on newts)	Yes; *Ta. granulosa*, *Ta. torosa* (*Ta. sierrae* likely, *Ta. rivulosa* unknown)	Yes; *Ta. sierrae*, *Ta. torosa* (*Ta. granulosa* likely)	convergence
	(Brodie 1968; Brodie et al 2002; Durso et al 2021)	(Brodie et al 2005; Wiseman & Pool 2007)	
geographic variation in newt predation	unknown	unknown	unknown
	N/A	N/A	
Whole Animal TTX resistance	Yes; organismal resistance in snakes from populations that consume newts	Yes; organismal resistance in snakes from populations that consume newts	convergence
	(Brodie 1968; Brodie & Brodie 1990, 1991)	(Brodie et al 2005; Feldman et al 2009)	
geographic variation in animal resistance	Yes; variation in organismal resistance within and across populations	Yes; variation in organismal resistance within and across populations	convergence
	(Brodie et al 2002; Hague et al. 2017, 2020)	(Reimche et al 2020; This Study)	
Skeletal Muscle Tissue TTX resistance	Yes; muscle resistance in snakes from populations that consume newts	Yes; muscle resistance in snakes from populations that consume newts	convergence
	(Geffeney et al 2002)	(This Study)	
geographic variation in muscle resistance	Yes; variation in muscle resistance across populations	Yes; variation in muscle resistance within and across populations	convergence
	(Geffeney et al 2002)	(This Study)	
Skeletal Muscle VGSC (Nav1.4) TTX resistance	Yes; VGSC replacements: DIV: I1556L, I1561V, G1566A, D1568N, G1569V	Yes; VGSC replacements: DIII: M1267T	convergence
	(Geffeney et al 2005)	(Feldman et al 2009; This Study)	
geographic variation in ***SCN4A*** alleles	Yes; VGSC alleles: Nav1.4+, Nav1.4V, Nav1.4VA, Nav1.4LVNV	No; single allele fixed across populations: Nav1.4T	divergence
	(Geffeney et al 2005; Feldman et al 2010; Hague et al 2017, 2020)	(This Study)	
Motor Neuron VGSC (Nav1.6) TTX resistance	Yes; VGSC replacements: DIII: D1393E; DIV: A1681G, D1684N, G1685Y	Yes; VGSC replacements: DIII: D1393E; DIV: A1681G, D1684N, G1685Y	shared ancestry
	(McGlothlin et al 2014, 2016)	(McGlothlin et al 2016)	
geographic variation in ***SCN8A*** alleles	unknown	No; single allele fixed across populations: Nav1.6EGNY	unknown
	N/A	(This Study)	
Sensory Neuron VGSC (Nav1.7) TTX resistance	Yes; VGSC replacements: DIV: I1709V	Yes; VGSC replacements: DIV: I1709V	shared ancestry
	(McGlothlin et al 2014, 2016)	(McGlothlin et al 2016)	
geographic variation in ***SCN9A*** alleles	uknown	No; single allele fixed across populations: Nav1.7V fixed	unknown
	N/A	(This Study)	
SCN4A **regulation associated with TTX resistance**	uknown	No; expression does not predict phenotype	unknown
	N/A	(This Study)	
geographic variation in ***SCN4A*** expression	uknown	No; expression does not differ within and across populations	unknown
	N/A	(This Study)	

Abbreviation: N/A, not applicable.

of *Th. couchii* will aid in our interpretation of phenotypic evolution and the process of convergence.

5 | CONCLUSIONS

We expect selection to shape convergence at the phenotypic surface, but as we move further down the chain of organization, convergence might arise from constraints on the physiological structures of adaptations, the underlying developmental programmes, the genetic architecture of traits or even bias in the production of genetic variation (Agrawal, 2017; Arnold, 1992; Brakefield, 2006; Brodie & Brodie, 2015; Christin et al., 2010; Feldman et al., 2012; Losos, 2011; Maynard Smith et al., 1985; Storz et al., 2019; Wake, 1991; Weinreich et al., 2006). On the other hand, we might see a greater role for contingency in phenotypic convergence the further we travel down the chain of organization because the developmental and genetic complexity of traits, the unique genomic histories of species, and the stochastic nature of mutation make it unlikely that convergent phenotypes will arise through the same physiological, developmental, and genetic routes (Christin et al., 2010; Losos, 2011; Wake, 1991). In addition, there may be more pathways that lead to functional phenotypes at lower levels (e.g., toxin-resistant muscle physiology) than exist at the next step. Here, as in other exceptional cases (e.g., Feldman et al., 2016; Mebs et al., 2016), we show that the evolution of toxin resistance may not always be constrained or predictable, and that convergence at the surface levels does not signify convergence at lower levels of organization, which may be more easily constructed in diverse ways and thus influenced by contingency.

AUTHOR CONTRIBUTIONS

C.R.F., E.D.B. Jr, E.D.B. III, M.E.P. and N.L. designed the study; C.R.F., E.D.B. III and J.S.R. field collected animals; E.D.B. Jr and C.R.F. collected whole-animal data; J.S.R. and R.E.dC. collected muscle data; C.R.F., J.S.R., R.E.dC. and J.W.M. collected sequence data; J.S.R. and C.R.F. collected qPCR data; J.S.R., R.E.dC., C.R.F., E.D.B. Jr, J.W.M. and K.S. analysed the data; C.R.F. and J.S.R. produced an initial draft; all authors contributed to the text and approved the final manuscript.

ACKNOWLEDGEMENTS

We thank CAF&W for permits to C.R.F., and USU and UNR IACUCs for approval of live animal protocols. We thank Mike Edgehouse, Kevin Wiseman and Bob Hansen for field advice, and Erica Ely, Rowan Feldman-Matocq and Matt Forister for aid with field collections. We are grateful to Gabrielle Blaustein, Haley Moniz, Vicki Thill, Amber Durfee, Kenzie Wasley, Taylor Disbrow, Sage Kruleski and Aubrey Smith for aid live animal care at UNR, and Haley Moniz, Vicki Thill, Kenzie Wasley, Taylor Disbrow and Jake Holland for invaluable work with the race track. We thank Josh Hallas, Jen Rippert, Mike Hague and the UNR Genomics Center for guidance on sequencing, Arielle Navarro for assistance with sequencing and myography, Daphne Cooper and Jacqueline Lopez for advice on RNA protocols, and Miriam Ba, Karla Hernández and Chase Fiore for help with qPCR protocols. We thank Angela Pitera for help with analyses and Josh Hallas for map aid. Lastly, we thank the UNR Evol Doers, especially Marjorie Matocq, Mike Logan, Jenny Ouyang, Josh Jahner, Valentina Alaasam, Haley Moniz, Danny Nielsen and Vicki Thill, for useful feedback and thoughtful discussions, and comments on the manuscript from Kerry Gendreau and Kait Malewicz (McGlothlin Laboratory). This work was supported by NSF grants to C.R.F. and N.L. (IOS-1355221), M.E.P. (DEB-1034686) and E.D.B. III (DEB-0922216 and DEB-1601296), and an NIH grant to N.L. (R01-HL146054).

DATA AVAILABILITY STATEMENT

We deposited all animals as voucher specimens in museums: herpetology collections of the California Academy Sciences (CAS); University of Texas, Arlington (UTA); University of Nevada, Reno (UNR). Phenotypic data are available on the Open Science Framework (OSF) digital repository: DOI 10.17605/OSF.IO/YUFZ9. All DNA sequences data are available on GenBank (MT415671 - MT415682, MT304461, MT432928 - MT433019, MT459158 - MT459171, MT460471 - MT460494; ON357429 - ON357572). All gene expression data are available on OSF: DOI 10.17605/OSF.IO/H9UT3.

ORCID

Jessica S. Reimche https://orcid.org/0000-0001-6536-7039
Robert E. del Carlo https://orcid.org/0000-0003-4845-7037
Edmund D. Brodie Jr https://orcid.org/0000-0002-5739-4747
Joel W. McGlothlin https://orcid.org/0000-0003-3645-6264
Karen Schlauch https://orcid.org/0000-0001-6916-8571
Michael E. Pfrender https://orcid.org/0000-0001-6861-0655
Edmund D. Brodie III https://orcid.org/0000-0001-9231-8347
Normand Leblanc https://orcid.org/0000-0002-1090-9432
Chris R. Feldman https://orcid.org/0000-0003-2988-3145

REFERENCES

Abal, P., Louzao, M. C., Antelo, A., Alvarez, M., Cagide, E., Vilarino, N., Vieytes, M. R., & Botana, L. M. (2017). Acute oral toxicity of tetrodotoxin in mice: Determination of lethal dose 50 (LD50) and no observed adverse effect level (NOAEL). *Toxins*, *9*(3), 6. https://doi.org/10.3390/toxins9030075

Abderemane-Ali, F., Rossen, N. D., Kobiela, M. E., Craig, R. A., Garrison, C. E., Chen, Z., Colleran, C. M., O'Connell, L. A., Du Bois, J., Dumbacher, J. P., & Minor, D. L. (2021). Evidence that toxin resistance in poison birds and frogs is not rooted in sodium channel mutations and may rely on "toxin sponge" proteins. *Journal of General Physiology*, *153*(9), e202112872. https://doi.org/10.1085/jgp.202112872

Agrawal, A. A. (2017). Toward a predictive framework for convergent evolution: Integrating natural history, genetic mechanisms, and consequences for the diversity of life. *American Naturalist*, *190*, S1–S12. https://doi.org/10.1086/692111

Akopian, A. N., Sivilotti, L., & Wood, J. N. (1996). A tetrodotoxin-resistant voltage-gated sodium channel expressed by sensory neurons. *Nature*, *379*(6562), 257–262. https://doi.org/10.1038/379257a0

Applied Biosystems. (2008). *Guide to performing relative quantitation of gene expression using real-time quantitative PCR*. Applied Biosystems. (Part Number 4371095 Rev B).

Arbuckle, K., de la Vega, R. C. R., & Casewell, N. R. (2017). Coevolution takes the sting out of it: Evolutionary biology and mechanisms of toxin resistance in animals. *Toxicon*, *140*, 118–131. https://doi.org/10.1016/j.toxicon.2017.10.026

Arnold, S. J. (1992). Constraints on phenotypic evolution. *American Naturalist*, *140*, S85–S107. https://doi.org/10.1086/285398

Backx, P. H., Yue, D. T., Lawrence, J. H., Marban, E., & Tomaselli, G. F. (1992). Molecular localization of an ion-binding site within the pore of mammalian sodium-channels. *Science*, *257*(5067), 248–251. https://doi.org/10.1126/science.1321496

Benn, S. C., Costigan, M., Tate, S., Fitzgerald, M., & Woolf, C. J. (2001). Developmental expression of the TTX-resistant voltage-gated sodium channels $Na_v1.8$ (SNS) and $Na_v1.9$ (SNS2) in primary sensory neurons. *Journal of Neuroscience*, *21*(16), 6077–6085.

Brakefield, P. M. (2006). Evo-devo and constraints on selection. *Trends in Ecology & Evolution*, *21*(7), 362–368. https://doi.org/10.1016/j.tree.2006.05.001

Brodie, E. D., III. (2009). Toxins and venoms. *Current Biology*, *19*, R931–R935. https://doi.org/10.1016/j.cub.2009.08.011

Brodie, E. D., III, & Brodie, E. D., Jr. (1990). Tetrodotoxin resistance in garter snakes: An evolutionary response of predators to dangerous prey. *Evolution*, *44*(3), 651–659. https://doi.org/10.1111/j.1558-5646.1990.tb05945.x

Brodie, E. D., III, & Brodie, E. D., Jr. (1991). Evolutionary response of predators to dangerous prey: reduction of toxicity of newts and resistance of garter snakes in Island populations. *Evolution*, *45*, 221–224.

Brodie, E. D., III, & Brodie, E. D., Jr. (1999). Costs of exploiting poisonous prey: Evolutionary trade-offs in a predator–prey arms race. *Evolution*, *53*, 626–631.

Brodie, E. D., III, & Brodie, E. D., Jr. (2015). Predictably convergent evolution of sodium channels in the arms race between predators and prey. *Brain, Behavior and Evolution*, *86*(1), 48–57. https://doi.org/10.1159/000435905

Brodie, E. D., III, Feldman, C. R., Hanifin, C. T., Motychak, J. E., Mulcahy, D. G., Williams, B. L., & Brodie, E. D., Jr. (2005). Parallel arms races between garter snakes and newts involving tetrodotoxin as the phenotypic interface of coevolution. *Journal of Chemical Ecology*, *31*(2), 343–356. https://doi.org/10.1007/s10886-005-1345-x

Brodie, E. D., Jr. (1968). Investigations on the skin toxin of adult rough-skinned newt, *Taricha granulosa*. *Copeia*, *2*, 307–313.

Brodie, E. D., Jr., Ridenhour, B. J., & Brodie, E. D., III. (2002). The evolutionary response of predators to dangerous prey: Hotspots and coldspots in the geographic mosaic of coevolution between garter snakes and newts. *Evolution*, *56*(10), 2067–2082.

Brown, M. S., & Mosher, H. S. (1963). Tarichatoxin: isolation and purification. *Science*, *140*, 295–296. https://doi.org/10.1126/science.140.3564.295

Bucciarelli, G. M., Lechner, M., Fontes, A., Kats, L. B., Eisthen, H. L., & Shaffer, H. B. (2021). From poison to promise: The evolution of tetrodotoxin and its potential as a therapeutic. *Toxins*, *13*, 517.

Cardall, B. L., Brodie, E. D., Jr., Brodie, E. D., III, & Hanifin, C. T. (2004). Secretion and regeneration of tetrodotoxin in the rough-skin newt (*Taricha granulosa*). *Toxicon*, *44*(8), 933–938. https://doi.org/10.1016/j.toxicon.2004.09.006

Catterall, W. A. (2012). Voltage-gated sodium channels at 60: structure, function and pathophysiology. *Journal of Physiology*, *590*(11), 2577–2589. https://doi.org/10.1113/jphysiol.2011.224204

Chen, C. L., Bharucha, V., Chen, Y. A., Westenbroek, R. E., Brown, A., Malhotra, J. D., Jones, D., Avery, C., Gillespie, P. J., Kazen-Gillespie, K. A., Kazarinova-Noyes, K., Shrager, P., Saunders, T. L., Macdonald, R. L., Ransom, B. R., Scheuer, T., Catterall, W. A., & Isom, L. L. (2002). Reduced sodium channel density, altered voltage dependence of inactivation, and increased susceptibility to seizures in mice lacking sodium channel β2-subunits. *Proceedings of the National Academy of Sciences of the United States of America*, *99*, 17072–17077.

Choudhary, G., Yotsu-Yamashita, M., Shang, L., Yasumoto, T., & Dudley, S. C., Jr. (2003). Interactions of the C^{-11} hydroxyl of tetrodotoxin with the sodium channel outer vestibule. *Biophysical Journal*, *84*, 287–294.

Christin, P. A., Weinreich, D. M., & Besnard, G. (2010). Causes and evolutionary significance of genetic convergence. *Trends in Genetics*, *26*(9), 400–405. https://doi.org/10.1016/j.tig.2010.06.005

Conway-Morris, S. (2003). The Cambrian "explosion" of metazoans and molecular biology: would Darwin be satisfied? *International Journal of Developmental Biology*, *47*(7–8), 505–515.

Cooper, T. F., Rozen, D. R., & Lenski, R. E. (2003). Parallel changes in gene expression after 20,000 generations of evolution in *Escherichia coli*. *Proceedings of the National Academy of Sciences of the United States of America*, *100*(3), 1072–1077. https://doi.org/10.1073/pnas.0334340100

Cowen, R. (2013). *History of life* (5th ed.). Wiley-Blackwell.

Currier, R. B., Calvete, J. J., Sanz, L., Harrison, R. A., Rowley, P. D., & Wagstaff, S. C. (2012). Unusual stability of messenger RNA in snake venom reveals gene expression dynamics of venom replenishment. *PLoS One*, *7*(8), e41888. https://doi.org/10.1371/journal.pone.0041888

Davis, R. W., Polasek, L., Watson, R., Fuson, A., Williams, T. M., & Kanatous, S. B. (2004). The diving paradox: new insights into the role of the dive response in air-breathing vertebrates. *Comparative Biochemistry and Physiology a-Molecular & Integrative Physiology*, *138*, 263–268.

Dobler, S., Wagschal, V., Pietsch, N., Dandouli, N., Meinzer, F., Romey-Glusing, R., & Schutte, K. (2019). New ways to acquire resistance: imperfect convergence in insect adaptations to a potent plant toxin. *Proceedings of the Royal Society B-Biological Sciences*, *286*(1908), 8. https://doi.org/10.1098/rspb.2019.0883

Du, Y. Z., Nomura, Y., Liu, Z. Q., Huang, Z. Y., & Dong, K. (2009). Functional expression of an arachnid sodium channel reveals residues responsible for tetrodotoxin resistance in invertebrate sodium channels. *Journal of Biological Chemistry*, *284*(49), 33869–33875. https://doi.org/10.1074/jbc.M109.045690

Feldman, C. R., Brodie, E. D., III, Brodie, E. D., Jr., & Pfrender, M. E. (2009). The evolutionary origins of beneficial alleles during the repeated adaptation of garter snakes to deadly prey. *Proceedings of the National Academy of Sciences of the United States of America*, *106*(32), 13415–13420. https://doi.org/10.1073/pnas.0901224106

Feldman, C. R., Brodie, E. D., Jr., Brodie, E. D., III, & Pfrender, M. E. (2010). Genetic architecture of a feeding adaptation: garter snake (Thamnophis) resistance to tetrodotoxin bearing prey. *Proceedings of the Royal Society B-Biological Sciences*, *277*(1698), 3317–3325. https://doi.org/10.1098/rspb.2010.0748

Feldman, C. R., Brodie, E. D., Jr., Brodie, E. D., III, & Pfrender, M. E. (2012). Constraint shapes convergence in tetrodotoxin-resistant sodium channels of snakes. *Proceedings of the National Academy of Sciences of the United States of America*, *109*(12), 4556–4561. https://doi.org/10.1073/pnas.1113468109

Feldman, C. R., Durso, A. M., Hanifin, C. T., Pfrender, M. E., Ducey, P. K., Stokes, A. N., Barnett, K. E., Brodie, E. D., 3rd, & Brodie, E. D., Jr. (2016). Is there more than one way to skin a newt? Convergent toxin resistance in snakes is not due to a common genetic mechanism. *Heredity*, *116*(1), 84–91. https://doi.org/10.1038/hdy.2015.73

ffrench-Constant, R. H. (1994). The molecular and population-genetics of cyclodiene insecticide resistance. *Insect Biochemistry and Molecular Biology*, *24*(4), 335–345. https://doi.org/10.1016/0965-1748(94)90026-4

Fozzard, H. A., & Lipkind, G. M. (2010). The tetrodotoxin binding site is within the outer vestibule of the sodium channel. *Marine Drugs*, *8*(2), 219–234. https://doi.org/10.3390/md8020219

Geffeney, S., Brodie, E. D., Jr., Ruben, P. C., & Brodie, E. D., III. (2002). Mechanisms of adaptation in a predator–prey arms race: TTX-resistant sodium channels. *Science*, *297*(5585), 1336–1339. https://doi.org/10.1126/science.1074310

Geffeney, S. L., Fujimoto, E., Brodie, E. D., III, Brodie, E. D., Jr., & Ruben, P. C. (2005). Evolutionary diversification of TTX-resistant sodium channels in a predator–prey interaction. *Nature*, *434*(7034), 759–763. https://doi.org/10.1038/nature03444

Geffeney, S. L., Williams, B. L., Rosenthal, J. J. C., Birk, M. A., Felkins, J., Wisell, C. M., Curry, E. R., & Hanifin, C. T. (2019). Convergent and parallel evolution in a voltage-gated sodium channel underlies TTX-resistance in the Greater Blue-ringed Octopus: *Hapalochlaena lunulata*. *Toxicon*, *170*, 77–84. https://doi.org/10.1016/j.toxicon.2019.09.013

Gendreau, K. L., Hornsby, A. D., Hague, M. T. J., & McGlothlin, J. W. (2021). Gene conversion facilitates the adaptive evolution of self-resistance in highly toxic newts. *Molecular Biology and Evolution*, *38*, 4077–4094.

Goldin, A. L. (2001). Resurgence of sodium channel research. *Annual Review of Physiology*, *63*, 871–894. https://doi.org/10.1146/annurev.physiol.63.1.871

Goldin, A. L. (2002). Evolution of voltage-gated Na^+ channels. *Journal of Experimental Biology*, *205*(5), 575–584.

Greene, R. R., & Feldman, C. R. (2009). Thamnophis atratus atratus Diet. *Herpetological Review*, *40*(1), 103–104.

Hague, M. T. J., Feldman, C. R., Brodie, E. D., Jr., & Brodie, E. D., III. (2017). Convergent adaptation to dangerous prey proceeds through the same first-step mutation in the garter snake *Thamnophis sirtalis*. *Evolution*, *71*(6), 1504–1518. https://doi.org/10.1111/evo.13244

Hague, M. T. J., Stokes, A. N., Feldman, C. R., Brodie, E. D., Jr., & Brodie, E. D., III. (2020). The geographic mosaic of arms race coevolution is closely matched to prey population structure. *Evolution Letters*, *4*, 317–332.

Hague, M. T. J., Toledo, G., Geffeney, S. L., Hanifin, C. T., Brodie, E. D., Jr., & Brodie, E. D., III. (2018). Large-effect mutations generate trade-off between predatory and locomotor ability during arms race co-evolution with deadly prey. *Evolution Letters*, *2*, 406–416.

Hallas, J. M., Parchman, T. L., & Feldman, C. R. (2022). Phylogenomic analyses resolve relationships among garter snakes (*Thamnophis*: Natricinae: Colubridae) and elucidate biogeographic history and morphological evolution. *Molecular Phylogenetics and Evolution*, *167*, 107374. https://doi.org/10.1016/j.ympev.2021.107374

Hanifin, C. T., Brodie, E. D., Jr., & Brodie, E. D., III. (2008). Phenotypic mismatches reveal escape from arms-race coevolution. *PLoS Biology*, *6*(3), 471–482. https://doi.org/10.1371/journal.pbio.0060060

Hanifin, C. T., & Gilly, W. F. (2015). Evolutionary history of a complex adaptation: tetrodotoxin resistance in salamanders. *Evolution*, *69*(1), 232–244. https://doi.org/10.1111/evo.12552

Harris, R. J., & Arbuckle, K. (2016). Tempo and Mode of the Evolution of Venom and Poison in Tetrapods. *Toxins*, *8*, 193.

Hille, B. (2001). *Ion channels of excitable membranes* (3rd ed.). Sinauer Associates.

Hindle, A. G. (2020). Diving deep: Mechanistic insights into the extreme physiology of Antarctic seals. *Integrative and Comparative Biology*, *60*, E103.

Huey, R. B., & Moody, W. J. (2002). Neuroscience and evolution. Snake sodium channels resist TTX arrest. *Science*, *297*, 1289–1290. https://doi.org/10.1126/science.1075987

Isom, L. L. (2001). Sodium channel beta subunits: Anything but auxiliary. *The Neuroscientist*, *7*(1), 42–54. https://doi.org/10.1177/107385840100700108

Jacob, F. (1977). Evolution and Tinkering. *Science*, *196*, 1161–1166.

Jayne, B. C. (1988). Muscular mechanisms of snake locomotion: An electromyographic study of the sidewinding and concertina modes of *Crotalus cerastes*, *Nerodia fasciata* and *Elaphe obsolete*. *Journal of Experimental Biology*, *140*, 1–33.

Johnson, W. E., Li, C., & Rabinovic, A. (2007). Adjusting batch effects in microarray expression data using empirical Bayes methods. *Biostatistics*, *8*(1), 118–127. https://doi.org/10.1093/biostatistics/kxj037

Jost, M. C., Hillis, D. M., Lu, Y., Kyle, J. W., Fozzard, H. A., & Zakon, H. H. (2008). Toxin-resistant sodium channels: parallel adaptive evolution across a complete gene family. *Molecular Biology and Evolution*, *25*(6), 1016–1024. https://doi.org/10.1093/molbev/msn025

Kearse, M., Moir, R., Wilson, A., Stones-Havas, S., Cheung, M., Sturrock, S., Buxton, S., Cooper, A., Markowitz, S., Duran, C., Thierer, T., Ashton, B., Meintjes, P., & Drummond, A. (2012). Geneious basic: An integrated and extendable desktop software platform for the organization and analysis of sequence data. *Bioinformatics*, *28*(12), 1647–1649. https://doi.org/10.1093/bioinformatics/bts199

Krause, U., Alflen, C., Steinmetz, M., Muller, M. J., Quentin, T., & Paul, T. (2015). Characterization of maturation of neuronal voltage-gated sodium channels SCN1A and SCN8A in rat myocardium. *Molecular and Cellular Pediatrics*, *2*(1), 5. https://doi.org/10.1186/s40348-015-0015-5

Leek, J. T., Johnson, W. E., Parker, H. S., Jaffe, A. E., & Storey, J. D. (2012). The sva package for removing batch effects and other unwanted variation in high-throughput experiments. *Bioinformatics*, *28*(6), 882–883. https://doi.org/10.1093/bioinformatics/bts034

Li, W. L., Cong, Q., Shen, J. H., Zhang, J., Hallwachs, W., Janzen, D. H., & Grishin, N. V. (2019). Genomes of skipper butterflies reveal extensive convergence of wing patterns. *Proceedings of the National Academy of Sciences of the United States of America*, *116*(13), 6232–6237. https://doi.org/10.1073/pnas.1821304116

Lopez-Santiago, L. F., Pertin, M., Morisod, X., Chen, C. L., Hong, S. S., Wiley, J., Decosterd, I., & Isom, L. L. (2006). Sodium channel β2 subunits regulate tetrodotoxin-sensitive sodium channels in small dorsal root ganglion neurons and modulate the response to pain. *Journal of Neuroscience*, *26*, 7984–7994.

Lorentz, M. N., Stokes, A. N., Rossler, D. C., & Lotters, S. (2016). Tetrodotoxin. *Current Biology*, *26*(19), R870–R872. https://doi.org/10.1016/j.cub.2016.05.067

Losos, J. B. (2011). Convergence, adaptation, and constraint. *Evolution*, *65*(7), 1827–1840. https://doi.org/10.1111/j.1558-5646.2011.01289.x

Losos, J. B. (2017). *Improbable destinies: fate, chance, and the future of evolution*. Riverhead Books.

Losos, J. B., Jackman, T. R., Larson, A., de Queiroz, K., & Rodriguez-Schettino, L. (1998). Contingency and determinism in replicated adaptive radiations of Island lizards. *Science*, *279*(5359), 2115–2118. https://doi.org/10.1126/science.279.5359.2115

Mahler, D. L., Ingram, T., Revell, L. J., & Losos, J. B. (2013). Exceptional convergence on the macroevolutionary landscape in Island lizard radiations. *Science*, *341*(6143), 292–295. https://doi.org/10.1126/science.1232392

Maier, S. K. G., Westenbroek, R. E., McCormick, K. A., Curtis, R., Scheuer, T., & Catterall, W. A. (2004). Distinct subcellular localization of different sodium channel alpha and beta subunits in single ventricular myocytes from mouse heart. *Circulation*, *109*(11), 1421–1427. https://doi.org/10.1161/01.cir.0000121421.61896.24

Matsui, T., Yamamori, K., Furukawa, K., & Kono, M. (2000). Purification and some properties of a tetrodotoxin binding protein from the blood plasma of kusafugu, *Takifugu niphobles*. *Toxicon*, *38*(3), 463–468. https://doi.org/10.1016/s0041-0101(99)00166-x

Maynard Smith, J., Burian, R., Kauffman, S., Alberch, P., Campbell, J., Goodwin, B., Lande, R., Raup, D., & Wolpert, L. (1985). Development constraints and evolution. *The Quarterly Review of Biology*, *60*(3), 265–287. https://doi.org/10.1086/414425

McCabe, T. M., & Mackessy, S. P. (2017). Evolution of resistance to toxins in prey. In A. Malhotra & P. Gopalakrishnakone (Eds.), *Evolution of venomous animals and their toxins* (Springer handbook of toxinology series) (pp. 47–65). Springer.

McGhee, G. R. (2011). *Convergent evolution: Limited forms most beautiful*. MIT Press.

McGlothlin, J. W., Chuckalovcak, J. P., Janes, D. E., Edwards, S. V., Feldman, C. R., Brodie, E. D., Pfrender, M. E., & Brodie, E. D. (2014). Parallel evolution of tetrodotoxin resistance in three voltage-gated sodium channel genes in the garter snake *Thamnophis sirtalis*. *Molecular Biology and Evolution*, *31*(11), 2836–2846. https://doi.org/10.1093/molbev/msu237

McGlothlin, J. W., Kobiela, M. E., Feldman, C. R., Castoe, T. A., Geffeney, S. L., Hanifin, C. T., Toledo, G., Vonk, F. J., Richardson, M. K., Brodie, E. D., Pfrender, M. E., & Brodie, E. D. (2016). Historical contingency in a multigene family facilitates adaptive evolution of toxin resistance. *Current Biology*, *26*(12), 1616–1621. https://doi.org/10.1016/j.cub.2016.04.056

Mebs, D., Yotsu-Yamashita, M., & Arakawa, O. (2016). The praying mantis (Mantodea) as predator of the poisonous red-spotted newt *Notophthalmus viridescens* (Amphibia: Urodela: Salamandridae). *Chemoecology*, *26*, 121–126.

Miller, S. P., Lunzer, M., & Dean, A. M. (2006). Direct demonstration of an adaptive constraint. *Science*, *314*(5798), 458–461. https://doi.org/10.1126/science.1133479

Namadurai, S., Yereddi, N. R., Cusdin, F. S., Huang, C. L. H., Chirgadze, D. Y., & Jackson, A. P. (2015). A new look at sodium channel beta subunits. *Open Biology*, *5*(1), 12. https://doi.org/10.1098/rsob.140192

Perry, B. W., Card, D. C., McGlothlin, J. W., Pasquesi, G. I., Adams, R. H., Schield, D. R., Hales, N. R., Corbin, A. B., Demuth, J. P., & Hoffmann, F. G. (2018). Molecular adaptations for sensing and securing prey and insight into amniote genome diversity from the garter snake genome. *Genome Biology and Evolution*, *10*, 2110–2129.

R Core Team. (2019). *R: A language and environment for statistical computing*. R Foundation Statistical Computing. http://www.R-project.org/

Reimche, J. S., Brodie, E. D., Stokes, A. N., Ely, E. J., Moniz, H. A., Thill, V. L., Hallas, J. M., Pfrender, M. E., Brodie, E. D., III, & Feldman, C. R. (2020). The geographic mosaic in parallel: Matching patterns of newt tetrodotoxin levels and snake resistance in multiple predator–prey pairs. *Journal of Animal Ecology.*, *89*, 1645–1657. https://doi.org/10.1111/1365-2656.13212

Ridenhour, B. J., Brodie, E. D., III, & Brodie, E. D., Jr. (2004). Resistance of neonates and field-collected garter snakes (*Thamnophis spp.*) to tetrodotoxin. *Journal of Chemical Ecology*, *30*(1), 143–154. https://doi.org/10.1023/B:JOEC.0000013187.79068.d2

Rogart, R. B., Cribbs, L. L., Muglia, L. K., Kephart, D. D., & Kaiser, M. W. (1989). Molecular-cloning of a putative tetrodotoxin-resistant rat heart Na^+ channel isoform. *Proceedings of the National Academy of Sciences of the United States of America*, *86*(20), 8170–8174. https://doi.org/10.1073/pnas.86.20.8170

Stayton, C. T. (2015). What does convergent evolution mean? The interpretation of convergence and its implications in the search for limits to evolution. *Interface Focus*, *5*, 20150039. https://doi.org/10.1098/rsfs.2015.0039

Stebbins, R. C. (2003). *Houghton Mifflin Co.* (3rd eds.). Wiley-Blackwell.

Stern, D. L. (2013). The genetic causes of convergent evolution. *Nature Reviews Genetics*, *14*(11), 751–764. https://doi.org/10.1038/nrg3483

Stocksley, M. A., Awad, S. S., Young, C., Lightowlers, R. N., Brenner, H. R., & Slater, C. R. (2005). Accumulation of Nav1 mRNAs at differentiating postsynaptic sites in rat soleus muscles. *Molecular and Cellular Neuroscience*, *28*, 694–702.

Storz, J. F. (2016). Causes of molecular convergence and parallelism in protein evolution. *Nature Reviews Genetics*, *17*(4), 239–250. https://doi.org/10.1038/nrg.2016.11

Storz, J. F., Natarajan, C., Signore, A. V., Witt, C. C., McCandlish, D. M., & Stoltzfus, A. (2019). The role of mutation bias in adaptive molecular evolution: insights from convergent changes in protein function. *Philosophical Transactions of the Royal Society of London B Biological Sciences*, *374*, 20180238.

Supple, M. A., Hines, H. M., Dasmahapatra, K. K., Lewis, J. J., Nielsen, D. M., Lavoie, C., Ray, D. A., Salazar, C., McMillan, W. O., & Counterman, B. A. (2013). Genomic architecture of adaptive color pattern divergence and convergence in *Heliconius* butterflies. *Genome Research*, *23*(8), 1248–1257. https://doi.org/10.1101/gr.150615.112

Tarvin, R. D., Santos, J. C., O'Connell, L. A., Zakon, H. H., & Cannatella, D. C. (2016). Convergent substitutions in a sodium channel suggest multiple origins of toxin resistance in poison frogs. *Molecular Biology and Evolution*, *33*(4), 1068–1081. https://doi.org/10.1093/molbev/msv350

Terlau, H., Heinemann, S. H., Stuhmer, W., Pusch, M., Conti, F., Imoto, K., & Numa, S. (1991). Mapping the site of block by tetrodotoxin and saxitoxin of sodium channel II. *FEBS Letters*, *293*, 93–96.

Tikhonov, D. B., & Zhorov, B. S. (2005). Modeling P-Loops domain of sodium channel: homology with potassium channels and interaction with ligands. *Biophysical Journal*, *88*, 184–197.

Tikhonov, D. B., & Zhorov, B. S. (2011). Possible roles of exceptionally conserved residues around the selectivity filters of sodium and calcium channels. *Journal of Biological Chemistry*, *286*, 2998–3006.

Ujvari, B., Casewell, N. R., Sunagar, K., Arbuckle, K., Wuster, W., Lo, N., O'Meally, D., Beckmann, C., King, G. F., Deplazes, E., & Madsen, T. (2015). Widespread convergence in toxin resistance by predictable molecular evolution. *Proceedings of the National Academy of Sciences of the United States of America*, *112*(38), 11911–11916. https://doi.org/10.1073/pnas.1511706112

Vaelli, P. M., Theis, K. R., Williams, J. E., O'Connell, L. A., Foster, J. A., & Eisthen, H. L. (2020). The skin microbiome facilitates adaptive tetrodotoxin production in poisonous newts. *Elife*, *9*, e53898. https://doi.org/10.7554/eLife.53898

Vandesompele, J., De Preter, K., Pattyn, F., Poppe, B., Van Roy, N., De Paepe, A., & Speleman, F. (2002). Accurate normalization of real-time quantitative RT-PCR data by geometric averaging of multiple internal control genes. *Genome Biology*, *3*(7), 12. https://doi.org/10.1186/gb-2002-3-7-research0034

Venkatesh, B., Lu, S. Q., Dandona, N., See, S. L., Brenner, S., & Soong, T. W. (2005). Genetic basis of tetrodotoxin resistance in pufferfishes. *Current Biology*, *15*(22), 2069–2072. https://doi.org/10.1016/j.cub.2005.10.068

Vlasenko, A. E., Kuznetsov, V. G., Malykin, G. V., Pereverzeva, A. O., Velansky, P. V., Yakovlev, K. V., & Magarlamov, T. Y. (2021). Tetrodotoxins secretion and voltage-gated sodium channel adaptation in the Ribbon Worm Kulikovia alborostrata (Takakura, 1898) (Nemertea). *Toxins*, *13*, 606.

Wake, D. B. (1991). Homoplasy: The result of natural selection, or evidence of design limitations? *American Naturalist*, *138*(3), 543–567. https://doi.org/10.1086/285234

Weinreich, D. M., Delaney, N. F., DePristo, M. A., & Hartl, D. L. (2006). Darwinian evolution can follow only very few mutational paths to fitter proteins. *Science*, *312*(5770), 111–114. https://doi.org/10.1126/science.1123539

Widmark, J., Sundstrom, G., Daza, D. O., & Larhammar, D. (2011). Differential evolution of voltage-gated sodium channels in tetrapods and teleost fishes. *Molecular Biology and Evolution*, *28*, 859–871.

Wilson, N. J., Stokes, A. N., Hopkins, G. R., Brodie, E. D., Jr., & Williams, C. R. (2014). Functional and physiological resistance of crayfish to amphibian toxins: tetrodotoxin resistance in the white river crayfish (*Procambarus acutus*). *Canadian Journal of Zoology*, *92*, 939–945.

Wiseman, K. D., & Pool, A. C. (2007). *Thamnophis couchii* (Sierra garter snake): Predator-prey interaction. *Herpetological Review*, *38*, 344.

Woods, R., Schneider, D., Winkworth, C. L., Riley, M. A., & Lenski, R. E. (2006). Tests of parallel molecular evolution in a long-term experiment with *Escherichia coli*. *Proceedings of the National Academy of Sciences of the United States of America*, *103*(24), 9107–9112. https://doi.org/10.1073/pnas.0602917103

Yoshida, S. (1994). Tetrodotoxin-resistant sodium channels. *Cellular and Molecular Neurobiology*, *14*(3), 227–244. https://doi.org/10.1007/bf02088322

Yotsu-Yamashita, M., Nagaoka, Y., Muramoto, K., Cho, Y., & Konoki, K. (2018). Pufferfish saxitoxin and tetrodotoxin binding protein (PSTBP) analogues in the blood plasma of the pufferfish *Arothron nigropunctatus*, *A. hispidus*, *A. manilensis*, and *Chelonodon patoca*. *Marine Drugs*, *16*(7), 10. https://doi.org/10.3390/md16070224

Yotsu-Yamashita, M., Yamaki, H., Okoshi, N., & Araki, N. (2010). Distribution of homologous proteins to puffer fish saxitoxin and tetrodotoxin binding protein in the plasma of puffer fish and among the tissues of Fugu pardalis examined by Western blot analysis. *Toxicon*, *55*, 1119–1124.

Zakon, H. H. (2012). Adaptive evolution of voltage-gated sodium channels: The first 800 million years. *Proceedings of the National Academy of Sciences of the United States of America*, *109*, 10619–10625. https://doi.org/10.1073/pnas.1201884109

Zakon, H. H., Jost, M. C., & Lu, Y. (2011). Expansion of voltage-dependent Na^+ channel gene family in early tetrapods coincided with the emergence of terrestriality and increased brain complexity. *Molecular Biology and Evolution*, *28*, 1415–1424.

Zimmer, T. (2010). Effects of tetrodotoxin on the mammalian cardiovascular system. *Marine Drugs*, *8*(3), 741–762. https://doi.org/10.3390/md8030741

SUPPORTING INFORMATION

Additional supporting information may be found in the online version of the article at the publisher's website.

How to cite this article: Reimche, J. S., del Carlo, R. E., Brodie, E. D., McGlothlin, J. W., Schlauch, K., Pfrender, M. E., Brodie, E. D., Leblanc, N., & Feldman, C. R. (2022). The road not taken: Evolution of tetrodotoxin resistance in the Sierra garter snake (*Thamnophis couchii*) by a path less travelled. *Molecular Ecology*, *31*, 3827–3843. https://doi.org/10.1111/mec.16538